applied nano

MDPI

Review

Zinc Oxide Nanoparticles for Skin Burn Wound Healing: A Comprehensive Review of Multifunctional Nanotherapeutic and Sensor-Integrated Platforms

Jharana Bajracharya [1], George Oguntala [1,*], Chinenye Anetekhai [2] and Blessing Odu [2]

[1] Department of Life and Sports Sciences, Birmingham City University, Birmingham B15 3TN, UK; jharana.bajracharya@mail.bcu.ac.uk
[2] Department of Nursing and Midwifery, Birmingham City University, Birmingham B15 3TN, UK; chinenye.anetekhai@bcu.ac.uk (C.A.); blessingoghenerukevwe.odu@bcu.ac.uk (B.O.)
* Correspondence: george.oguntala@bcu.ac.uk

Abstract

Burns injuries present critical health and care challenges and remain one of the leading causes of preventable morbidity globally. The pathophysiology of burns injuries combines barrier disruption, dysregulated inflammation and biofilm-driven polymicrobial infection. Zinc oxide nanoparticles (ZnO NP) offer unique, multi-functional capabilities of broad-spectrum antimicrobial, pro-regenerative zinc (II) ion sources and an intrinsic transducer that is piezoelectric, photoresponsive and pH-responsive. This paper presents a comprehensive review of ZnO NP for the treatment of skin burns injuries with a focus on its multifunctional nanotherapeutic and sensor-integrated platforms. A structured literature search of PubMed, Scopus, Web of Science, Embase and IEEE Xplore covering the period 2015 to 2025 was conducted to identify and consolidate relevant pre-clinical and clinical evidence on ZnO-based and sensor-integrated burn wound platforms. From the survey across hydrogels, electrospun nanofibers, films, sprays, and three-dimensional bio-printed constructs, it is established that ZnO formulations achieve 60–95% wound closure by day 14 versus 30–55% for untreated controls, with 3–7 log10 colony-forming-unit reductions and minimum inhibitory concentrations of 8–256 micrograms per millilitre against multidrug-resistant pathogens. Wound healing is driven by sustained Zn^{2+} release, reactive-oxygen-species-mediated bactericidal action, matrix-metalloproteinase-9 modulation, vascular-endothelial-growth-factor and hypoxia-inducible-factor-1-alpha angiogenesis, and nuclear-factor-kappa-B suppressed inflammation. Emerging closed-loop sensor-integrated dressings deliver real-time wound pH, temperature, and matrix-metalloproteinase-9 readout coupled to near-field-communication actuated on-demand zinc release. Clinical translation is affected by several factors such as dose-dependent cytotoxicity associated with excessive ROS generation or dissolution, limited standardisation of green-synthesis methodologies, batch-to-batch variability in nanoparticle physicochemical properties and limited clinical trial data. ZnO-based theranostic platforms hold practical clinical translation potentials provided reproducible GMP-scale synthesis, long-term biocompatibility validation and comprehensive regulatory classification is systematically addressed.

Keywords: nanomaterial; nanoparticle; skin burns; wound healing; theranostic dressings; zinc oxide

Academic Editors: Dimitrios Bikiaris and Hans Bäumler

Received: 12 June 2026
Revised: 18 August 2026
Accepted: 21 August 2026
Published: 1 September 2026

1. Introduction

The skin constitutes the largest organ of the human body and serves as a mechanical, immunological and homeostatic barrier against pathogens, ultraviolet radiation and dehydration [1,2]. Burn injuries caused by exposure to elevated temperature from various sources including heat, flame, scalds, electricity, chemicals, friction, or radiation affects the homeostatic barrier resulting in local and systemic processes with severity ranging in depth and total body surface area (TBSA). In a recent World Health Organisation (WHO) report, it is estimated that approximately 11 million burn injuries occur each year, with more than 180,000 burn injury-related deaths concentrated in low and middle-income countries [3–5]. In another report from Global Burden of Disease (GBD), it is estimated that about 13 million persons experienced severe burns, and 235 million experienced minor burns in 2021, and that demographic growth and ageing will significantly impact absolute case numbers by 2050 [6–8]. Beyond acute mortality, survivors of partial and full-thickness burns face long-term morbidity from hypertrophic scarring, contracture, psychological sequelae, and the cumulative cost of repeated reconstructive surgery [9,10].

The pathophysiology of burn wounds is conceptualised through Jackson's three concentric zones: a central zone of coagulation (irreversible necrosis), a surrounding zone of stasis characterised by reduced tissue perfusion that remains potentially viable and can be salvaged through timely and appropriate therapeutic intervention [11]. Burn injuries disrupt the normal wound healing cascaded by prolonging the inflammatory phase, resulting in sustained expression of pro-inflammatory cytokines, including tumour necrosis factor-α (TNF-α), interleukin-1β (IL-1β), and interleukin-6 (IL-6), together with persistent neutrophil infiltration. Concurrently, the wound microbiome evolves from early colonisation by Gram-positive organisms, predominantly *Staphylococcus aureus* and coagulase-negative Staphylococcus spp., to later predominance of Gram-negative pathogens such as Pseudomonas aeruginosa, Acinetobacter baumannii, and Klebsiella pneumoniae, frequently accompanied by Candida albicans biofilm formation [12–14]. Biofilm extracellular polymeric substances shield embedded organisms behind diffusion barriers and quorum-sensing-regulated tolerance phenotypes that elevate apparent minimum inhibitory concentrations (MICs) by up to three orders of magnitude, which in turn, drives high incidence of burn wound sepsis and multi-organ failure [15,16]. Burn wound healing progresses through four temporally overlapping phases including haemostasis, inflammation, proliferation and remodelling, with each process characterised by distinct cellular and molecular events and potential intervention points for ZnO nanoparticles (NPs) occurring throughout the healing process as illustrated in Figure 1. In Figure 1, it is worth noting that only antimicrobial activity in the inflammatory phase has meaningful translational support among the phase-specific roles highlighted shown. However, the remaining proliferative and remodelling actions of ZnO NPs are predominantly preclinical and have not been established as clinical outcomes in burn wound management.

Conventional burn management includes surgical debridement, split-thickness skin grafting, topical antimicrobial agents such as silver sulfadiazine, mafenide acetate, and chlorhexidine, and silver-containing dressings such as Mepilex Ag, Acticoat, and Aquacel Ag [12,13]. Although these interventions remain the standard of care, their effectiveness is increasingly challenged by two major limitations. First, silver-based agents, chlorhexidine, and some topical antibiotics exhibit cytotoxic effects on keratinocytes and fibroblasts, which impair the cellular migration required for re-epithelialisation and create a well-recognised trade-off between antimicrobial activity and tissue regeneration [17,18]. Second, antimicrobial resistance is increasing, with reports of silver-resistant *Enterobacteriaceae* and mupirocin-resistant *Staphylococcus aureus* in burn intensive care units [19]. In addition, autologous split-thickness skin grafting is constrained by donor-site morbidity and limited

donor skin availability in patients with burns involving more than 40–50% TBSA, which elucidates the need for off-the-shelf multifunctional wound therapies [13,20].

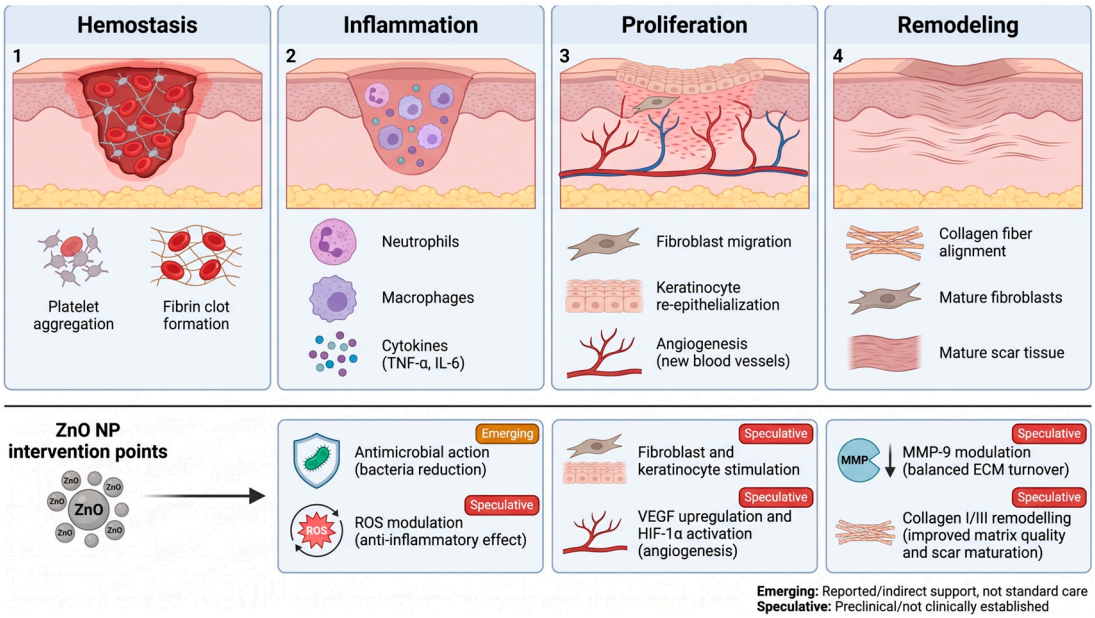

Figure 1. Conceptual schematic of burn wound healing phases and proposed ZnO NP intervention points (Created in BioRender. https://BioRender.com/rrpds9v, accessed on 20 August 2026).

Nanotechnology offers viable solution as nanoscale materials, typically within the 1–100 nm region, exhibit distinct therapeutic characteristics due to their size-dependent physicochemical properties that is conversely lacking in high surface-to-volume or bulk materials [21,22]. This is because at the nanoscale, a high surface-to-volume ratio increases surface reactivity which improve catalysis and adsorption, subject to reconstruction, faceting and passivation. Nanoscale defects and non-stoichiometry enhance the redox and charge-transfer kinetics which reshapes optical and electronic responses, enabling design windows that bulk solids cannot reach [23,24]. NP are engineered to mimic features of the native extracellular matrix, deliver sustained or stimulus-responsive payloads, modulate angiogenesis, oxidative stress, and collagen deposition, and traverse cellular and vascular barriers more efficiently than conventional formulations [25–27]. Across the metallic, metal-oxide, polymeric, and composite NP families, metal-oxide NP based on Zinc (Zn), Titanium (Ti), Copper (Cu), Iron (Fe) and Cerium (Ce) have gained intense attention for wound care due to their combination of antimicrobial activity, redox modulation, and biocompatibility characteristics [28–31].

Zn is a key trace element involved in numerous physiological processes including DNA synthesis, gene transcription, enzymatic regulation and tissue repair. ZnO NPs are widely employed in biomedical and antimicrobial applications due to their wide band-gap of approximately 3.36 eV and unique optical, electrical, catalytic, and biological characteristics [32,33]. These properties contribute to photocatalytic activity, reactive oxygen species (ROS) generation, and tunable surface interactions that collectively enhance antimicrobial performance. Compared with bulk ZnO (~2 μm), nanoscale ZnO particles (10–50 nm) exhibit enhanced antibacterial efficacy owing to their increased surface reactivity and reduced particle size [34,35]. Current evidence indicates that their antimicrobial activity arises through multiple concurrent mechanisms, including ROS generation, Zn^{2+} ion release, electrostatic membrane disruption, protein dysfunction and inhibition of bacterial biofilm formation [34,35]. The biological effects are highly dependent on nanoparticle size, morphology, surface defects, concentration, and environmental conditions such as pH and light

exposure. Although ZnO NP exhibit favourable thermal stability and broad-spectrum antimicrobial activity, their biocompatibility remains strongly dose- and exposure-dependent, as excessive ROS production and Zn^{2+} dissolution may induce oxidative stress, mitochondrial dysfunction, inflammatory responses, and cytotoxicity in mammalian cells [25,35,36].

A key contribution of the present work is the systematic integration of sensor-engineering dimension of ZnO for wound healing. To the best of the author's knowledge, no previous review on ZnO for burn wound care consolidates ZnO effect as both nanotherapeutic and intrinsic transducer (e.g., piezoelectric, photoresponsive and pH-responsive) for sensor-integrated theranostic dressings, which constitutes the primary novelty of the present study. The present work has four objectives: (i) synthesise preclinical and early clinical evidence on ZnO-based burn wound platforms published between 2015 and 2025; (ii) develop a quantitative benchmarking framework comparing ZnO with key alternative nanomaterials; (iii) establish a taxonomy for sensor-integrated theranostic ZnO dressings; and (iv) outline a regulatory and translational roadmap linking material design, manufacturing, and clinical implementation. The remainder of the article is organised as follows: Section 2 describes the literature search methodology and scope of the review. Section 3 presents the literature review across eight subsections from pathophysiology through clinical translation; Section 4 discusses the existing clinical potentials and articulates the future directions of ZnO, while highlighting key open gaps. Section 5 draws conclusions and translational priorities.

2. Methodology

The review is conducted using structured literature search strategy to ensure comprehensive and reproducible search of published works on ZnO nanoparticle-based burn wound healing platforms and sensor-integrated theranostic dressings. The scope of the review was defined by the following eligibility criteria:

Target Population: Human or animal subjects with thermal, chemical, electrical, or radiation burn wounds of any depth and TBSA, plus in vitro models of burn wound microbiology and re-epithelialisation.

Intervention of Interest: ZnO nanoparticle-containing formulations, including hydrogels, nanofibers, films, sprays, injectables, 3D-bioprinted constructs, and sensor-integrated theranostic dressings, irrespective of synthesis route such as chemical, physical, or biogenic.

Comparators considered: Untreated controls, vehicle-only controls, standard-of-care antiseptics including silver sulfadiazine, chlorhexidine and mafenide acetate, commercial silver dressings, metal and metal-oxide NP materials.

Outcomes of Interest: Quantitative wound closure, re-epithelialisation kinetics, colony-forming-unit (CFU) reductions and MICs, scar metrics (Vancouver Scar Scale, hypertrophy index), angiogenesis, collagen I/III ratio, cytotoxicity (HaCaT, NHDF, BJ-5ta IC50) and sensor performance, in terms of limit of detection, response time, drift.

Study Design: The study design includes in vitro, in vivo studies restricted to mammalian burn models for rodent, lagomorph and porcine; non-mammalian models were not considered. Clinical studies (case series, phase I/II/III) were also included, whereas reviews and meta-analyses were excluded from the primary analysis but consulted for cross-reference and citation tracking. The literature search cover various publications published between January 2015 and December 2025 across five major databases and repositories including PubMed/MEDLINE, Scopus, Web of Science Core Collection, Embase, and IEEE Xplore. The IEEE Xplore database was used to capture sensor and electronics literature typically missed by biomedical-only searches. Search strings combined ("Zinc Oxide" OR "ZnO") AND ("nanoparticle" OR "nanorod" OR "nanowire" OR "nanofiber") AND ("burn" OR "thermal injury" OR "wound healing") AND, for the sensor sub-search,

("biosensor" OR "piezoelectric" OR "smart dressing" OR "theranostic" OR "impedimetric" OR "amperometric" OR "surface acoustic wave" OR "SAW"). The retrieved articles were screened by title and abstract for relevance to meet the eligibility criteria defined above, while full-text articles were assessed for final inclusion. Reference lists of included studies and relevant review articles were hand-searched to identify additional records not captured by the database searches. Reported quantitative outcomes including wound-closure percentages, MICs, and CFU counts) are presented as descriptive ranges synthesised narratively across heterogeneous primary studies and not as statistically pooled estimates and between-study differences in models, particle characteristics, and assay conditions preclude formal meta-analysis. The overall study-selection workflow from database identification through screening and eligibility assessment to narrative synthesis is summarised in Figure 2.

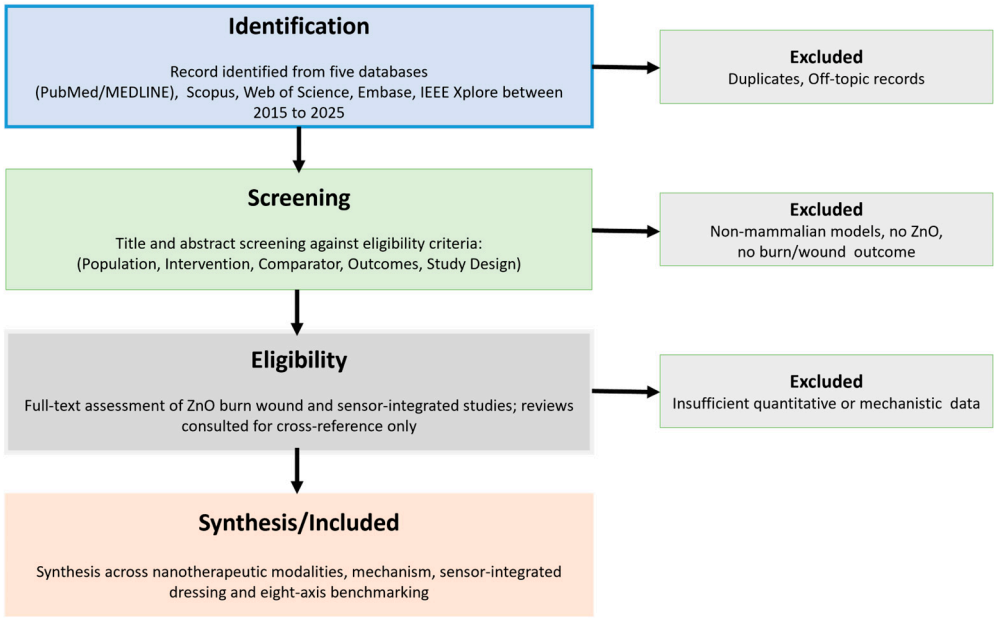

Figure 2. Overview of structured literature search and study selection workflow applied in the study.

3. Literature Review

Burn injuries affect both the skin and underlying tissue layers and may be classified as superficial, partial-thickness (superficial or deep), or full-thickness depending on the depth of dermal involvement [37,38]. Persistent inflammation, infection, scarring, and delayed re-epithelialisation are characteristic complications, and effective management hinges on three concurrent imperatives: preventing infection, supporting epithelial proliferation, and maintaining a moist, mechanically protective wound environment [39]. Inadequate care produces bleeding, infection, prolonged convalescence, and elevated treatment cost [40]. Because no absolute remedy exists for severe burns, identifying therapies that simultaneously combat infection and accelerate regenerative processes is a clinical priority [41].

Nanotherapeutic approaches have demonstrated significant potential to enhance wound healing through the use of diverse nanomaterials [42]. NP are generally defined as particles with dimensions between 1 and 100 nm [3]. The high surface area-to-volume ratio of NPs makes them particularly suitable for targeted drug delivery and loading of therapeutic agents [21,22]. Shape-controlled NP, including nanowires, nanorings, nanotubes, and nanotetrapods, can be synthesised using various methods such as chemical vapor deposition, electrodeposition, and thermal evaporation [23,24]. In accordance with standard nanomedicine classification, NP are categorised by composition as metallic, metal-

oxide, polymeric, lipid-based, carbon-based and hybrid systems. Metallic NP have broad applications in nano-pharmaceuticals, medical diagnostics, and biomedicine, including drug delivery, wound healing, cancer therapy, imaging, tissue engineering, diabetes management, and cosmetics [26,27,43]. Their dimensions overlap with those of biological structures such as proteins, DNA, and viruses, facilitating cellular and vascular interactions that can enhance therapeutic efficacy [44]. Additionally, important pathophysiological processes including oxidative stress, inflammation, angiogenesis and collagen deposition can be modulated by nanoparticles, which demonstrates the potential of nanotechnology for advanced burn wound therapy.

Chronic wound management has witnessed significant increase in the use of metal nanoparticles, metal oxide nanoparticles, polymeric nanomaterials (nanoparticles, nanofibers, nano emulsion), and other nanotherapeutics due to their antimicrobial and regenerative properties [28,29]. Metallic and metal-oxide nanomaterials including Ag, Au, ZnO, aluminium oxide, iron oxide, titanium dioxide, CoO, and gallium-based NP exhibit antibacterial activity that supports wound repair. However, due to the difference in cytotoxicity, stability, and cost, recent studies have focused on metal-oxide nanoparticles such as ZnO, which exhibit a more favourable cytotoxicity profile than silver toward mammalian keratinocytes and fibroblasts at comparable antibacterial doses [30,31].

Owing to their distinctive optical, electrical, and biological properties, ZnO NPs are widely applied in biomedical and antimicrobial applications due to their broad band-gap semiconductor (3.36 eV) [32,33]. The strong antibacterial activity of ZnO NPs diminishes the possibility of infection, while the narrow size promotes angiogenesis, cell proliferation, collagen remodelling, and sustained zinc release during wound healing [45]. The generation of reactive oxygen species governs the size-dependent antimicrobial mechanism of ZnO with nanosized ZnO ranging between 10 and 50 nm. Recent studies established ZnO NP exhibit antibacterial, antioxidant, and wound-healing properties to improve treatment of burn wounds. A few application domains of ZnO NP is illustrated in Figure 3.

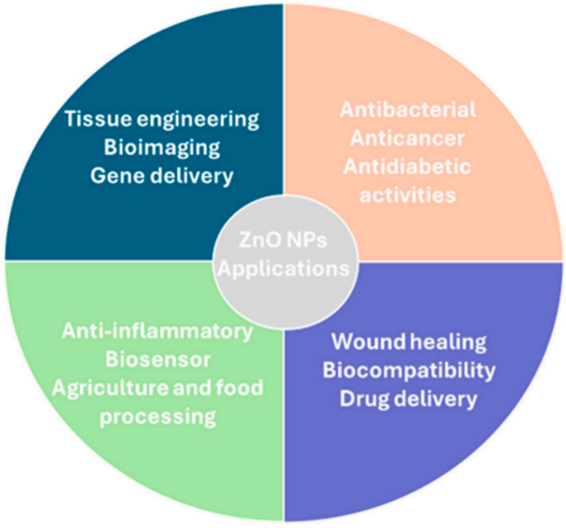

Figure 3. Applications of ZnO NPs is adapted from Xiao et al. [25], published under the CC BY 4.0 licence.

In therapeutic applications, ZnO NP creams formulated with calendula extract enhance fibroblast proliferation in Wistar rat burn models, indicating a synergistic effect that augments wound healing alongside the NP' intrinsic antimicrobial and antioxidant properties [46]. Similarly, magnesium-doped ZnO NPs green-synthesised via *Ferulago angulata* extract have demonstrated efficacy in accelerating the healing of second-degree

burn wounds [47]. Beyond acute burns, ZnO NPs are extensively investigated across diverse wound modalities, including diabetic ulcers, chronic wounds, and acute trauma as illustrated in Figure 4.

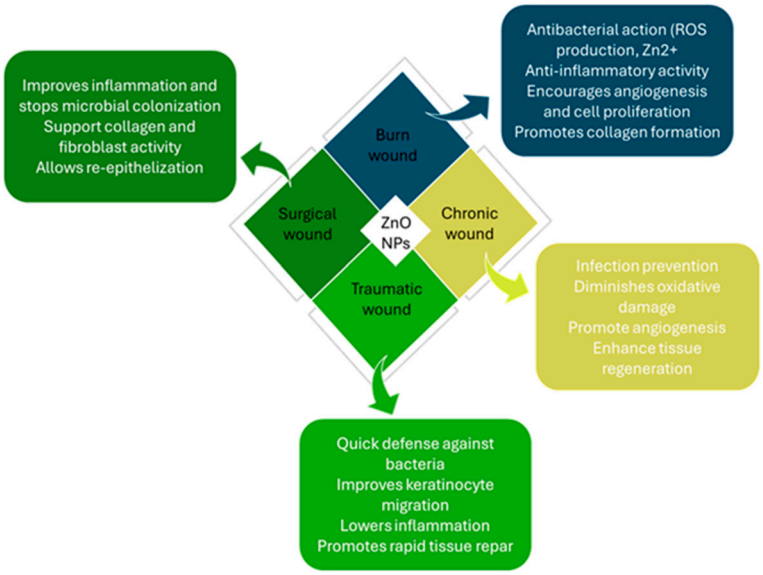

Figure 4. ZnO NP applications in different wound healing applications, adapted from Xiao et al. [25], published under the CC BY 4.0 licence.

Experimental studies show that incorporating ZnO NPs into hydrogels, nanofibers, biofilms, and bioactive dressings significantly accelerates healing by enhancing collagen deposition, re-epithelialisation, and antimicrobial protection [48]. Chitosan dressings loaded with Ag/ZnO nanocomposites exhibit potent antibacterial activity and promote tissue repair by upregulating collagen synthesis [48]. Mechanistically, ZnO NPs modulate the healing cascade by stimulating angiogenesis, mitigating oxidative stress, and regulating cytokine expression [49,50]. Despite the promising therapeutic features of ZnO NPs, their clinical translation faces several biological and operational challenges. Biological challenges include high-dose cytotoxicity, particle instability, systemic biosafety concerns and wound heterogeneity [13,30,49,50], whereas operational challenges such as high manufacturing costs, stringent regulatory pathways, and translational variations between animal models and human physiology. Additionally, due to nanomaterial toxicity is highly dependent on size, shape, stability, and dosage, optimising formulation parameters, establishing standardisation protocols, and developing real-time wound monitoring systems are critical to ensure safe and effective nanotherapy-based wound care [13,30,42,51].

3.1. Nanotherapeutic Modalities

ZnO NPs are highly effective in burn care; however, their therapeutic efficacy relies heavily on the delivery vehicle. Different nanotherapeutic modalities have been developed to optimise localised bioavailability, achieve sustained release and prevent nanoparticle aggregation [52]. These nanotherapeutic modalities include nano-loaded wound dressings, topical gels, hybrid nanostructures, nanocomposite hydrogels, electrospun nanofibers, polymer-based films/patches, and injectable systems [53].

ZnO NP-integrated gels and dressings are effective in wound care [54] and often supplement with cell proliferation promoters, moisture-retention agents and antimicrobials. Nanocomposite hydrogels such as chitosan- or alginate-based matrices maintain a moist wound environment and facilitate controlled drug delivery. A keratin-chitosan bandage functionalised with ZnO NPs stimulates collagen synthesis and cell adhesion to accelerate

tissue closure [55]. Topical burn creams frequently combine ZnO NPs with vitamins or plant extracts often results in improved therapeutic outcomes [56–58]. Additionally, flexible, microporous chitosan hydrogel-ZnO NPs composite bandages exhibit robust antibacterial properties and accelerate tissue regeneration by improving moisture retention and cellular proliferation [59], whereas green-synthesised ZnO NPs such as those mediated by *Ocimum americanum* leaf extract offer an eco-friendly approach to treat burn infections due to their potent phytochemical-enhanced antibacterial and antioxidant activities [60].

Advanced structural matrices further optimise burn wound healing by improving the local wound environment to support tissue regeneration. Electrospun nanofibers mimic the ECM architecture to promote cell adhesion, cell increase and tissue repair while providing an effective protective barrier [61,62]. Injectable hydrogels conform to irregular wound beds to enable uniform coverage and sustained delivery of antimicrobial agents, whereas polymer films and patches provide a breathable protective barrier that facilitates wound contraction. Among these platforms, hydrogels exhibit viable potentials for burn dressings due to their ability to maintain a moist wound environment, promote tissue regeneration, and provide controlled release of therapeutic agents, resulting in reduced infection risk [63,64]. Table 1 provide a summary of the various nanotherapeutic modalities for burns wound healing strategies.

Table 1. Comparison of ZnO NP-based burn wound healing strategies.

Modality	Techniques	Effects on Wound Healing	Limitations	References
Green-synthesised ZnO NPs mediated by plants	Generates ROS and disrupts microbial membranes; exhibits anti-inflammatory and pro-angiogenic activities to drive fibroblast growth.	Improve tissue regeneration, accelerate epithelialisation and reduce infection rates.	Phytochemical composition variability, dose-dependent cytotoxicity and lack of extensive clinical validation.	[38,58,65–67]
Biopolymer nanocomposite hydrogels, e.g., keratin, chitosan, ZnO	Provides broad-spectrum antibacterial action; matrix facilitates cell adhesion, maintains moisture, and prolongs drug delivery.	Improves burn wound contraction and enhance granulation tissue synthesis, and decrease bacterial load.	Complex manufacturing, scalability and reproducibility bottleneck, and potential high-concentration toxicity.	[37,55,68,69],
Terpenoid-stabilised ZnO NPs	Scavenges excess ROS and modulates oxidative stress pathways; increases NP stability while normalising oxidative imbalances.	Mitigate oxidative damage, efficient for inflammation management and rapid burn tissue repair.	Batch-to-batch terpenoid variations, limited in vivo profiling, and undefined long-term safety.	[70–73]
Wheat-gluten films treated with vita-mins and ZnO/AgNP nanocomposite	Matrix provides sustained nutrient and NP release; leverages dual metal antibacterial synergy alongside vitamin-driven ROS control.	Decrease infection, enhance collagen deposition, and accelerate in vivo burn contraction.	Formulation complexity, unpredictable release kinetics, and a need for large-animal validation.	[74–77]
ZnO-based biocomposite dressings	Drives antimicrobial action through concurrent ROS generation and Zn^{2+} ion release within supportive nanomaterials to exploit its biopolymer matrix.	Improve wound closure rates and minimise infection susceptibility.	Delineation of full antimicrobial spectra against diverse clinical pathogens is still ongoing.	[78–83]
ZnO/TiO_2 nanoparticle antimicrobial agents	Positive surface charges promote attachment to negative bacterial walls; generates ROS to disrupt biofilms and compromise bacterial viability.	Effective for eradication of biofilm-producing *S. aureus* and MRSA; lowers wound bioburden.	TiO_2 requires light activation for optimal performance; sparse in vivo data; activity varies by size/dose.	[84–88]
ZnO NP-loaded thixotropic Xymedone gels	Xymedone upregulates metabolic activity and tissue repair; thixotropic formulation improves spreadability, adhesion and sustained release.	Better granulation and epithelialisation, improves wound contraction and high patient compliance via optimised rheology.	Limited comparative clinical research; therapeutic performance is highly formulation-dependent.	[89–93]

3.2. Nanotherapeutic Technologies

ZnO NPs are compared with other metal complementary therapeutic properties for effective burn wound treatments [94]. Ag NPs exhibit broad-spectrum antimicrobial activity but are limited by dose-dependent cytotoxicity and limited regenerative capacity [95]. Au NPs possess excellent biocompatibility and drug-delivery capabilities with minimal intrinsic antibacterial activity [96,97]. TiO_2 NPs demonstrate antimicrobial activity, but their efficacy typically depends on ultraviolet light activation, which limit its clinical applicability [98,99]. Chemical synthesis methods including sol–gel, precipitation, and hydrothermal techniques, enable precise control over ZnO NPs size, morphology and crystallinity [42,100]. However, chemical-synthesised ZnO NPs often exhibit high surface reactivity which increase cytotoxicity, necessitating surface functionalisation before biomedical application [45,101]. Conversely, plant-mediated green synthesis enhances biocompatibility and surface bioactivity when incorporated with naturally derived phytochemicals. Plant-mediated green synthesis is often limited by its process standardisation and batch-to-batch reproducibility [102,103]. To improve nanoparticle stability and therapeutic performance, ZnO NPs are commonly incorporated into polymeric scaffolds and hydrogels to provide structural support, enhance mechanical properties and enable controlled Zn^{2+} ion release [104]. Electrospun poly(lactic-co-glycolic acid) (PLGA) or silk fibroin nanofibers, as well as schizophyllan (SPG)-modified bacterial cellulose scaffolds, are ZnO NPs delivery systems that mimics the natural architecture of ECM to support cell adhesion and tissue regeneration [105,106].

The high susceptibility of burn wounds to microbial infection makes the antibiofilm activity of ZnO NPs critical. ZnO NPs disrupt bacterial biofilms due to their biocompatibility, antibacterial properties and ability to inhibit biofilms using ROS [107,108]. The antibacterial efficacy of ZnO NPs is strongly influenced by its nanoscale size which enables its higher membrane and cytoplasmic accumulation than larger particles [109]. The integration of ZnO NPs with chitosan hydrogels, collagen matrices or cellulose-based scaffolds preserve the antimicrobial activity while improving tissue remodelling [78,110]. Controlled-release nanotherapeutic systems further optimise this balance by maintaining sustained antimicrobial activity while facilitating tissue repair [111]. Raguvaran et al. demonstrated that sodium alginate/gum acacia hydrogels containing ZnO NPs significantly improves the adhesion and proliferation of fibroblasts, thereby facilitating healing [112].

ZnO NP-coated wound dressings have been established to inhibits the viability of bacteria in chronic wounds within 6 h and maintaining antimicrobial efficacy for up to 3 days. To further enhance therapeutic performance, ZnO NP-doped biopolymer scaffolds are used to enhance the efficacy of ZnO NP-based dressings [113]. Karahaliloglu et al. and Soubhagya et al. demonstrated enhanced antibacterial activity in chitosan/silk sericin scaffolds loaded with ZnO NP and 3D chitosan/pectin/ZnO-NPs films are non-toxic, suitable to growth of fibroblasts [114,115].

Table 2 highlight four key delivery techniques of ZnO NPs in burn wound management including plant-mediated green synthesis, electrospun nanofiber incorporation, hydrogel and scaffold composite and polymer-based nanocomposites. It is worth noting that the tabulated values used for the analysis are representative figures from cited primary studies and are indicative rather than standardised head-to-head measurements. Plant-mediated delivery technique offers cost-effective, bio-compatible synthesis using phytochemical reducing and capping agents. However, plant-mediated delivery technique is affected by variety of factors including batch-to-batch variability, undefined dose—toxicity relationships and absence of clinical validation. Electrospun nanofiber combined with ZnO NPs technique exhibit strong antibacterial efficacy and good biocompatibility, and provides high surface area-to-volume scaffolding. However, the functionality of electrospun nanofiber

delivery strategy is limited by sub-optimal degradation kinetics, photo-dependent antimicrobial activation and nanoparticle aggregation. Hydrogel and scaffold composite offer improved tissue regeneration signalling and maintain moist wound micro-environment suitable for re-epithelialisation. Keratin-chitosan, alginate and cellulose nanocomposites provide mechanical support and moisture retention but is affected by delimitating factors such as mechanical stability under physiological loading and GMP-scalable manufacturing.

Table 2. Comparative overview of ZnO NP delivery techniques for burn wound healing.

Technique	Materials	Features	Key Limitations	Reference
Unformulated/Bare ZnO NPs	Plant extract (Aloe vera, moringa oleifera, camellia sinensis, azadirachta indica) as stabilising and reducing agents	Dual antimicrobial (ROS generation, Zn^{2+} release) and pro-angiogenic wound-healing action, eco-friendly and single-step synthesis	Toxicity uncertainty, batch-to-batch variability, lack of clinical trials, shallow mechanistic understanding.	[57,102,103,116,117],
Electrospun nanofibers matrices	Chitosan, silk fibroin, cellulose acetate, polycaprolactone (PCL), polyvinyl alcohol (PVA) nanofibers	High surface area-to-volume ratio; sustained ZnO release, ECM-mimetic architecture, strong antibacterial action and good biocompatibility	Slow degradation kinetics, minimal antimicrobial effect in absence of ZnO without light exposure, NP aggregation at high loading and limited in vivo validation.	[106,118–120]
Hydrogel and 3D porous scaffolds	Alginate, chitosan, PVA, hyaluronic acid, carbopol, polyethylene glycol (PEG) hydrogels; Collagen, silk-sericin, gelatin, bacterial cellulose scaffolds with ZnO NPs	Moist wound micro-environment, swelling-controlled Zn^{2+} release, improved re-epithelialisation, injectable formats and thermo-responsive variants. Interconnected porosity supports cell infiltration and neovascularisation; structural tissue-regeneration template; sustained antimicrobial defence; tuneable pore architecture	Weak mechanical strength under physiological loading, residual cytotoxicity at high ZnO concentrations are key limitations of ZnO NP with hydrogel. 3D scaffold on the other hand faces critical limitations including complex fabrication, batch reproducibility challenges, incomplete degradation profiling, gaps in clinical translation and GMP scalability.	[90,100,105,121–123]
Nanocomposites loaded with ZnO NPs	Keratin–chitosan, alginate/hyaluronic acid, cellulose nanocrystal, PCL/gelatin hybrid composites	Multi-material functionality, robust antimicrobial efficacy, improved tissue regeneration, moist wound environment, tuneable mechanical and release properties	ZnO toxicity issues, mechanical-stability under dynamic wound condition, standardisation and scalability challenges.	[55,74,79,124]

3.3. ZnO Physiochemistry and Structure Activities

ZnO crystallises predominantly in the wurtzite hexagonal structure (space group P63mc, lattice parameters a = 3.25 angstrom, c = 5.21 angstrom), with alternative cubic zinc blende and rock salt polymorphs accessible only under non-equilibrium or high-pressure conditions [125,126]. The wurtzite lattice of ZnO is non-centrosymmetric which generate spontaneous polarisation along the c-axis that underpins its piezoelectric behaviour, whilst

the chemically distinct Zn-terminated (0001) polar, O-terminated (000-1) polar and (10-10) non-polar facets differentially govern surface reactivity, protein corona formation, ROS and biological membrane adhesion [69,127]. Three intrinsic point defects are commonly associated with the physicochemical and biological behaviour of ZnO including oxygen vacancies (V_0), zinc interstitials (Zn_i), and zinc vacancies (V_Z_n). Among these, oxygen vacancies and zinc interstitials are frequently linked to enhanced surface reactivity and reactive oxygen species (ROS) generation. Singly ionised oxygen vacancies $(V_0{}^+)$ can serve as electron donor sites that facilitate interfacial electron transfer to adsorbed molecular oxygen, promoting the formation of superoxide radicals $(O_2{}^-)$. Subsequent redox reactions at the ZnO surface may also generate hydroxyl radicals (•OH), which contribute to the antibacterial and wound-healing activity of ZnO NP. The electron paramagnetic resonance (EPR) signals near g ≈ 2.003 are widely reported as indicative of oxygen-vacancy-related defect states in ZnO, although assignment of this signal can vary depending on synthesis conditions and defect complexity [128]. The optical band gap of ZnO is typically expressed using the Tauc relation for a direct allowed transition characteristic of wurtzite ZnO as:

$$(\alpha h\upsilon)^2 = A(h\upsilon - E_g) \quad (1)$$

where α is the absorption coefficient, which is a function of wavelength (λ), h is Planck constant, υ is frequency, A is the proportionality constant, E_g is the optical band gap of ZnO and n is Tauc exponent. Bulk wurtzite ZnO possess a direct band gap of 3.37 eV (approx.) at room temperature. For ZnO NP with crystallite sizes below approximately 10 nm, a blue shift in E_g, typically around 50–200 meV relative to bulk ZnO occur as a result of quantum confinement [129]. Figure 5 present a structure–property–function relationships of ZnO NPs.

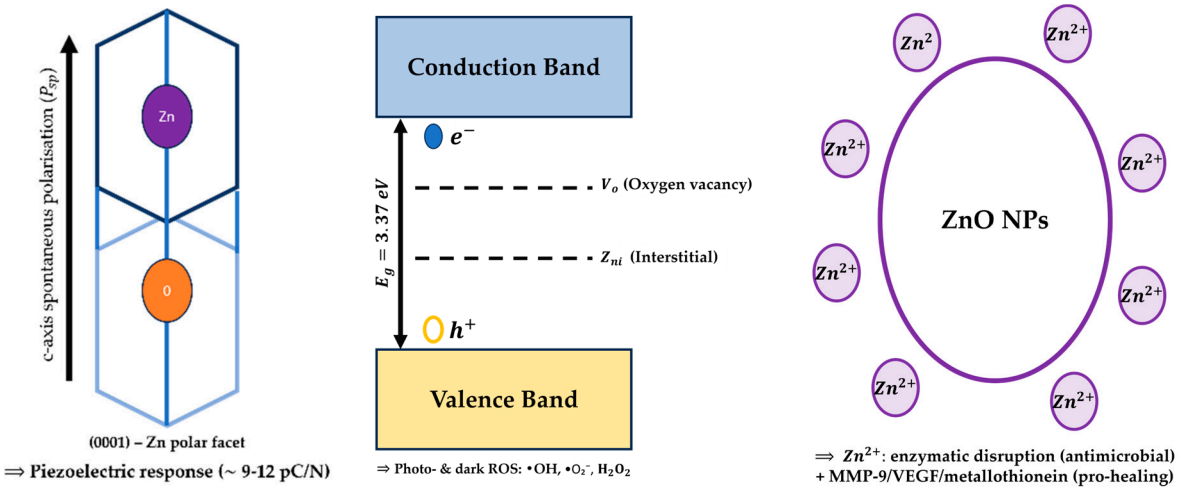

Figure 5. Structure–property–function relationships of ZnO NPs. (**a**) Non-centrosymmetric wurtzite lattice, (**b**) band structure and defect chemistry, (**c**) surface dissolution and ion release.

Figure 5a highlights the non-centrosymmetric wurtzite lattice and c-axis spontaneous polarisation underpinning piezoelectric behaviour of ZnO, whereas Figure 5b demonstrates the ≈3.37 eV wide direct band gap and intrinsic point defects for oxygen vacancies and zinc interstitials which governs the photocatalytic and dark ROS generation; and Figure 5c demonstrates the surface dissolution release of Zn^{2+} for antimicrobial and pro-healing activity.

3.4. Synthesis Routes

The synthesis route is a key determinant of ZnO NP size, morphology, crystallinity, defect density, surface chemistry and consequently, its biological activity. ZnO NPs are generally synthesised using three approaches including chemical, physical, and biogenic (green) methods. Chemical methods including ding sol–gel, co-precipitation, hydrothermal, solvothermal, microwave-assist and sonochemical synthesis, enable precise control of particle characteristics and produce high-purity nanoparticles at relatively low cost. Chemical method often suffers from residual solvents, surfactants and precursor ions which affects the ZnO NPs biocompatibility if not mitigated. Physical methods such as ball milling, laser ablation, chemical vapor deposition (CVD) and thermal evaporation, produce highly crystalline NPs with minimal chemical contamination. Due to the complexity of physical method strategies, these methods require high energy input and specialised equipment. Green or biogenic synthesis uses plant extracts such as Aloe vera, *Calendula officinalis*, *Ferulago angulata*, *Ocimum americanum*, and *Camellia sinensis*, fungi or bacteria, with naturally occurring phytochemicals, including polyphenols, flavonoids and terpenoids which function as reducing and stabilising agents. Biogenic synthesis approach generally improves biocompatibility and antioxidant properties but is affected by batch-to-batch variability, which limits the process standardisation and regulatory approval [45–47,130].

Several preclinical studies have demonstrated the therapeutic potential of biogenically synthesised ZnO NPs for burn wound repair. ZnO NP creams formulated with Calendula officinalis extract significantly improves fibroblast proliferation in second-degree burn wounds in Wistar rats which indicate the combined effects of ZnO and bioactive phytochemical capping agents [46]. In [47], Mg-doped ZnO NPs synthesised using Ferulago angulata extract were characterised and evaluated for second-degree burn healing to demonstrate the feasibility of combining green synthesis with elemental doping to improve biological performance. Beyond burn injuries, ZnO NPs have also been extensively investigated in diabetic ulcers, chronic wounds and acute traumatic injuries, which support its broad wound-healing potentials [48]. To improve reproducibility and facilitate clinical translation, continuous-flow microreactor systems with controlled phytochemical inputs have emerged as a promising strategy for good manufacturing practice (GMP)-compatible green synthesis of ZnO NPs, preserving the biocompatibility advantages of plant-mediated synthesis while reducing batch-to-batch variability [131]. Table 3 presents the comparison of the various synthesis routes on ZnO NPs.

Table 3. Comparison of synthesis route for biomedical-grade ZnO NPs.

Route	Typical Size (nm)	Morphology	Throughput	Energy Demand	Reproducibility	Biomedical Suitability	References
Continuous-flow microreactor (biogenic feed)	10–60	Spherical	High	Low	High (engineered)	Excellent (GMP-compatible)	[131]
Sol–gel	10–80	Spherical, irregular	High	Low	High	Good (residual alkoxides)	[132]
Co-precipitation	20–100	Spherical, rod	Very high	Low	High	Good (counter-ion residue)	[133]
Hydrothermal	10–200	Rod, flower, tetrapod	High	Moderate	High	Excellent (clean)	[134]
Solvothermal	5–150	Plate, rod, polyhedral	Moderate	Moderate-high	High	Moderate (organic solvents)	[135]

Table 3. *Cont.*

Route	Typical Size (nm)	Morphology	Throughput	Energy Demand	Reproducibility	Biomedical Suitability	References
Microwave-assisted	5–50	Spherical, rod	Moderate	Low (rapid)	High	Good	[136]
Sonochemical	5–40	Spherical, plate	Moderate	Moderate	Moderate	Good	[137]
Ball milling	50–500	Irregular	High	High	Moderate	Limited (contamination)	[138]
Laser ablation	5–50	Spherical	Low	Very high	High	Excellent (clean)	[139]
CVD	10–100	Rod, wire, tetrapod	Low	Very high	High	Good	[140]
Biogenic/green (plant extract)	10–100	Spherical, hexagonal	Variable	Low	Low-moderate	Excellent (intrinsic capping)	[46,47,57,60]

3.5. Antimicrobial and Pro-Healing Mechanisms

ZnO NPs exhibit strong potential for burn wound management because they combine antimicrobial activity with tissue-regenerative functions within a single biomaterial platform. The therapeutic performance of ZnO NPs arise from a combination of surface-mediated redox activity, controlled Zn^{2+} ion release, and the modulation of cellular wound-healing pathways [141]. Several complementary mechanisms contribute to antibacterial activities of ZnO NPs including ROS generation, membrane interactions and ion release. The surface-mediated generation of ROS occurs under both UV illumination and, to a markedly lesser extent, physiological dark conditions, where dark ROS output is typically on the order of ~10–30% of the UV-illuminated level [142,143]. Because burn wounds are not routinely UV-irradiated, the clinically dominant antibacterial contributions in vivo are Zn^{2+} dissolution and defect-mediated dark ROS instead of photocatalytic ROS. The principal ROS associated with ZnO include hydroxyl radicals, superoxide radicals, hydrogen peroxide and the singlet oxygen [142,143].

ZnO NP exert antibacterial effects through direct membrane interactions, where defect-rich (positively charged) ZnO surfaces electrostatically interact with negatively charged bacterial cell envelopes, which lead to membrane destabilisation, increased permeability and eventual leakage of intracellular components. NP below approximately 50 nm effectively penetrate biofilm extracellular polymeric substances to achieve closer contact with bacterial membranes, which subsequently enhance the antibacterial efficacy [144]. The controlled release of Zn^{2+} ions further contribute to antimicrobial activity, as dissolved Zn^{2+} disrupts the bacterial enzymatic system, interfere with membrane transport, alters the intracellular redox balance and impair metabolic homeostasis. Smaller ZnO NPs generally demonstrate stronger antibacterial activity than larger particles due to their greater specific surface area, higher defect density and increased cellular interaction. Notably, ZnO NPs within the 10–50 nm size range typically exhibit improved antibacterial performance than micron-scale ZnO particles [32,33,109]. Beyond size, morphology is a critical determinant of activity: rod-shaped ZnO NPs often outperform spherical particles of comparable size, owing to their high-er aspect ratio and the greater proportion of reactive polar (0001) facets, which enhance ROS generation and membrane interaction. ZnO NP contribute directly to tissue repair and wound regeneration, and modulates matrix metalloproteinase (MMP)-2 and MMP-9 activity, which supports rebalancing of extracellular matrix degradation and collagen deposition within the wound bed. ZnO treatment is associated with increased vascular endothelial growth factor (VEGF) expression and drive angiogenesis

through modulation of hypoxia-responsive signalling pathways, including HIF-1α [145]. The antimicrobial and pro-healing mechanism pathways of ZnO is illustrated in Figure 6.

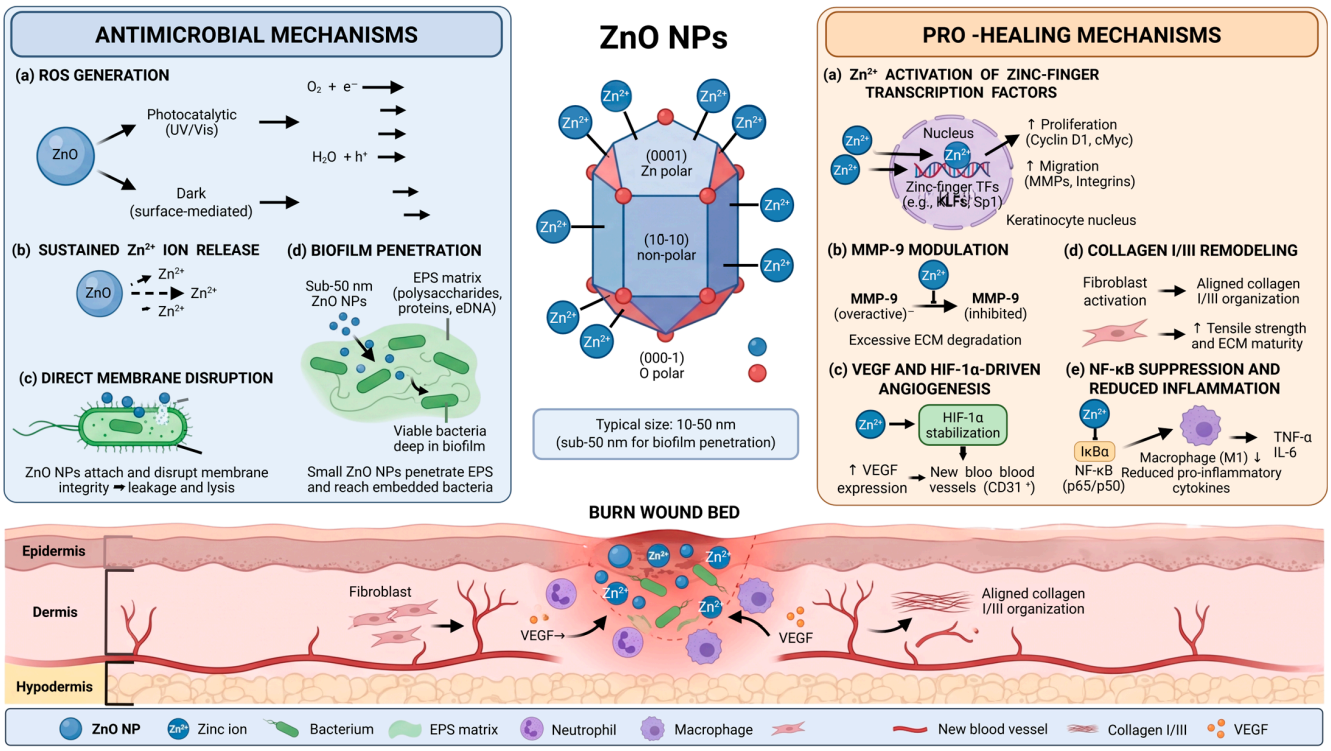

Figure 6. Antimicrobial and pro-healing mechanisms of ZnO NP at the burn wound bed (Created in BioRender. https://BioRender.com/5xtcs49, accessed on 20 August 2026).

ZnO-based dressings also exhibit improved collagen maturation, promoting type I/type III collagen ratio more characteristic of mechanically-stable repaired tissue [48–50]. Additionally, at sub-cytotoxic concentrations, ZnO NP attenuate NF-κB signalling, reduce macrophage production of pro-inflammatory cytokines such as TNF-α and IL-6 which support the resolution of the inflammatory phase [146]. Table 4 summarises the specific pathways, biomarkers and net biological effect of ZnO NPs for burn wound healing.

Table 4. Mechanism summary for ZnO NP in burn wound healing.

Specific Pathway	Biomarker	Net Biological Effect	Mechanism Class	References
Biofilm penetration (sub-50 nm NPs)	Confocal LIVE/DEAD biofilm imaging	Penetration of EPS and killing of embedded organisms	Antimicrobial	[109,144]
VEGF/HIF-1-alpha angiogenesis	CD31 vessel density; VEGF ELISA	Two- to four-fold vessel density increase vs. controls	Pro-healing	[145]
NF-kappaB suppression	TNF-alpha, IL-6 ELISA	Faster resolution of inflammatory phase	Pro-healing	[25,146]
Photocatalytic and dark ROS generation	•OH, O_2•$^-$, H_2O_2 (EPR, fluorescent probes)	Membrane lipid peroxidation, protein and DNA oxidation	Antimicrobial	[32–34,147]
Direct membrane disruption	Cell-leakage assay (260 nm), TEM membrane imaging	Loss of membrane integrity, cytoplasmic spillage	Antimicrobial	[148]

Table 4. *Cont.*

Specific Pathway	Biomarker	Net Biological Effect	Mechanism Class	References
Sustained Zn^{2+} release	ICP-MS Zn quantisation; thiol depletion	Zn-finger protein dyshomeostasis, Fenton synergy	Antimicrobial	[149]
Zn^{2+} activation of Zn-finger transcription factors	Metallothionein, Sp1, GLI expression	Keratinocyte proliferation and migration	Pro-healing	[150]
MMP-2/-9 modulation	Zymography; MMP-9 ELISA	Rebalanced proteolysis vs. deposition	Pro-healing	[151]
Collagen I/III ratio shift	Picrosirius red histology	Mature scar with adequate tensile strength	Pro-healing	[48–50]

3.6. Nanotherapeutic Delivery Platform

ZnO NP-incorporated gels, hydrogels, nanofibers, films and composite dressings are widely investigated for burn and chronic wound management due to their combined antimicrobial activity and tissue-regenerative properties [54]. Polymeric wound matrices based on chitosan, alginate, gelatin, keratin and polyvinyl alcohol provides a hydrated microenvironment to facilitate gas exchange, exudate absorption and controlled therapeutic delivery while simultaneously serve as carriers for ZnO NPs. ZnO NP-loaded nanocomposite hydrogels maintain moisture balance, enable sustained Zn^{2+} release and prolong antimicrobial activity, which support re-epithelialisation and extracellular matrix remodelling. Keratin–chitosan composite dressings containing ZnO nanoparticles have been reported to improve fibroblast adhesion, collagen deposition and keratinocyte proliferation leading to accelerated wound closure and tissue regeneration [55]. ZnO NPs have also been incorporated into topical burn formulations with bioactive phytochemicals, vitamins, and plant-derived reducing agents to enhance antioxidant capacity, biocompatibility, and antibacterial efficacy [56–58]. Flexible microporous chitosan/ZnO nanocomposite hydrogels exhibit potent antibacterial activity in both in vitro and in vivo wound models through the combined effects of reactive oxygen species (ROS) generation, Zn^{2+} ion release, bacterial membrane disruption, and promotion of a moist environment conducive to cellular proliferation [59]. Plant-mediated synthesis has attracted increasing interest because phytochemical capping agents may improve colloidal stability, biocompatibility, and antioxidant activity while potentially reducing nanoparticle-associated cytotoxicity. Electrospun ZnO-containing nanofibers further mimic the extracellular matrix through their high porosity and surface area, promoting cell adhesion, nutrient transport, and tissue regeneration while providing sustained antimicrobial protection [61,62]. Additionally, injectable ZnO-loaded hydrogels conform to irregular wound geometries and enable localised sustained therapeutic delivery, whereas ZnO-containing polymer films and patches provide breathable barriers which limit microbial contamination and support wound contraction. Collectively, these multifunctional ZnO nanocomposite platforms combine structural support, controlled therapeutic release, antimicrobial activity, and regenerative functionality, making them promising candidates for next-generation burn wound dressings [63,64].

3.7. Sensor-Integrated and Theranostic ZnO Dressing

The non-centrosymmetric wurtzite crystal structure of ZnO imparts piezoelectric properties, with effective piezoelectric coefficients of approximately 9–12 pC/N reported for high-quality ZnO nanostructures. These properties enable piezoelectric nanogenerators (PENGs) that convert wound-associated mechanical deformation into localised electrical stimulation to generate electrical outputs ranging from millivolts to volts depending

on device architecture and applied strain. Such electrical stimulation has been shown to promote fibroblast and keratinocyte migration through electrotaxis and may also enhance antibacterial activity at the wound–dressing interface [152,153]. ZnO nanowire- and nanorod-based photodetectors exhibit rapid ultraviolet (UV) photoresponses near the intrinsic band-edge wavelength of ~370 nm, while visible-light detection can be achieved through defect engineering or heterostructure design, supporting real-time phototherapy dosimetry [154]. Flexible ZnO-based surface acoustic wave (SAW) biosensors have also demonstrated sensitive detection of proteins and small molecules with sub-hertz frequency resolution [155]. In addition, defect-mediated photoluminescence in ZnO is pH-sensitive within the 5.5–9 range relevant to wound exudate, providing a label-free optical readout of healing status [156]. Table 5 illustrate the sub-architecture of sensor-integrated ZnO for burn wound dressing. The reported tabulated metrics are representative values from cited primary studies. Readers are referred to interpret these metrics as indicative rather than standardised head-to-head measurements.

Table 5. Sensor-integrated ZnO burn wound dressing.

Sub Architecture	Sensing Element	Analyte	Detection Range	Response Time	Integration	Reference
Intrinsic PENG	ZnO nanorod array on PDMS	Self-powered electrical stimulation (electrotaxis, antibacterial)	Output ~1–3 V at body motion	millisecond	Self-powered	[153]
Intrinsic photodetector	ZnO nanowire	UV (~370 nm) and visible irradiance	10 nW/cm^2–mW/cm^2	sub-sec	Wired/NFC	[154]
Intrinsic SAW	ZnO film on $LiNbO_3$/flexible	Protein binding	Sub-Hz frequency shift	sec	Wireless RF	[155]
Intrinsic PL	ZnO defect emission	Wound pH	pH 5.5–9	sec	Optical fibre/camera	[156]
Extrinsic enzymatic	ZnO nanorod	Glucose	1 microM–10 mM	sec	Amperometric	[157]
Extrinsic enzymatic	ZnO/lactate oxidase	Lactate (hypoxia)	0.1–25 mM	sec	Amperometric	[158]
Extrinsic aptasensor	ZnO nanorod/aptamer	MMP-9	sub-ng/mL	sec–min	Impedimetric	[159]
Extrinsic uricase	ZnO nanostructure/uricase	Uric acid (oxidative stress)	microM	seconds	Amperometric	[160]
Wireless e-skin	ZnO multi-analyte panel	pH^+ temperature + MMP-9	as above	seconds	NFC/BLE smartphone	[161]
Closed-loop theranostic	ZnO-Au/NIR/NFC	Trigger Zn^{2+} release on demand	N/A	seconds	Microcontroller-driven	[162]

ZnO nanostructured electrodes provide a high specific surface area, favourable biocompatibility, versatile surface functionality for enzymes and aptamers, and efficient electron-transfer pathways, making them attractive for wearable biosensing applications. Several medical devices which utilise the ZnO nanostructured electrodes configuration include amperometric glucose biosensors with micromolar limits of detection (LoD), lactate biosensors for assessing tissue hypoxia, matrix metalloproteinase-9 (MMP-9) aptasensors with sub-ng/mL LoD for monitoring chronic wound inflammation, uric acid sensors as indicators of oxidative stress, and integrated temperature and oxygen sensors for comprehensive wound assessment. Flexible platforms fabricated on polydimethylsiloxane (PDMS), Ecoflex, or thermoplastic polyurethane (TPU) substrates using screen-printed silver and ZnO inks integrated with near-field communication (NFC) tags or Bluetooth Low Energy (BLE) modules have also been developed to enable wireless transmission of multiplexed wound data to smartphones or clinical monitoring systems. Battery-less devices powered

by ZnO-based PENGs are particularly attractive for ambulatory burn care and home monitoring due to their reduced onboard power usage. A key feature of theranostic dressing is closed-loop coupling, where the sensor readings initiate the microcontroller decision to drive one or more actuators to deliver the right therapy at the right time in accordance with the wound chemistry [162]. The full layered architecture of the closed-loop theranostic ZnO for smart wound dressing is illustrated in Figure 7.

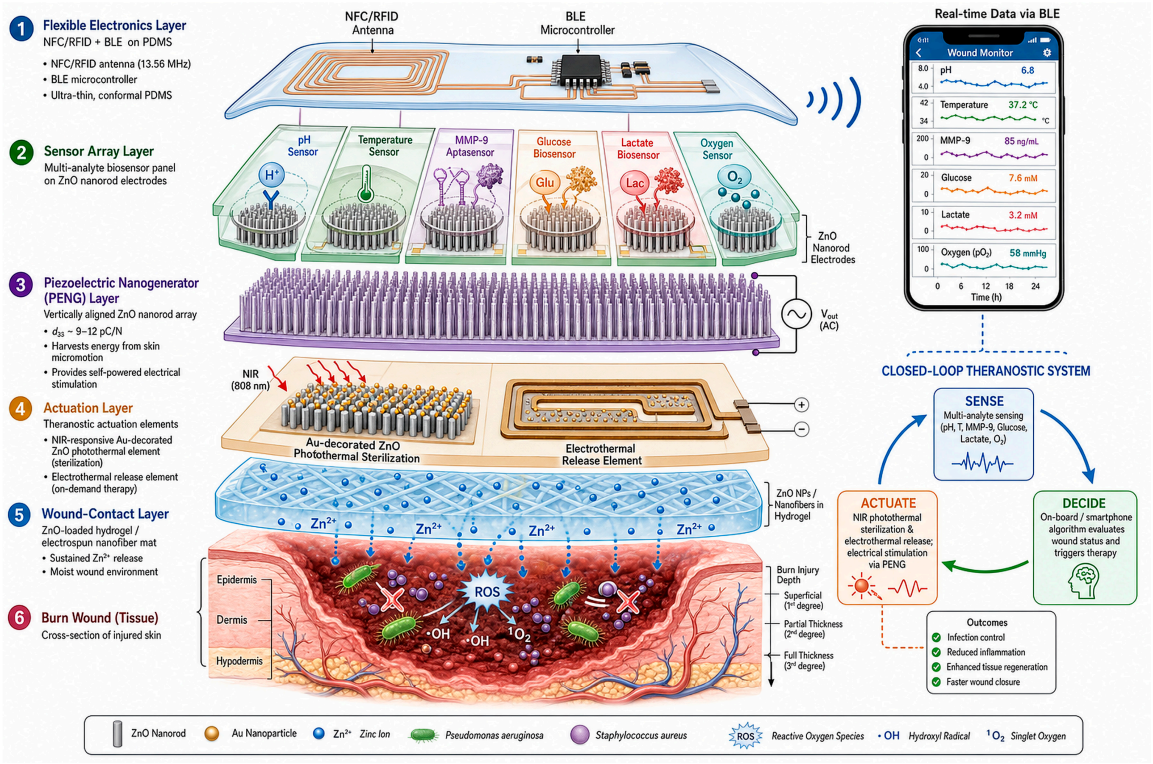

Figure 7. Layered architecture of closed-loop theranostic ZnO smart wound dressing.

3.8. Comparative Analysis of ZnO Against Other Metal and Metal-Oxide NP

The section evaluates key metal and metal-oxide NPs that are most frequently benchmarked against ZnO for wound-care applications, with a detailed eight-axis comparison provided in Table 6.

Table 6. Comparison of eight-axis benchmarking of metal and metal-oxide NPs against ZnO.

Axis	Antibacterial MIC Range (microg/mL)	Log10 CFU Reduction (Typical)	IC50 Fibro-Blast (microg/mL)	Day-14 Wound Closure (%)	Intrinsic Sensing Modality	Materials Cost (Relative)	Regulatory Status	AMR Development Risk	References
ZnO	8–256	3–7	50–150	60–95	Piezo/ photo/ pH-PL	Low	GRAS for Zn; multiple OTC ZnO products	Low (multimodal mechanism)	[163–165]
Ag NPs	0.5–32	5–9	5–25	50–85	None	Moderately high	Multiple Ag dressings cleared	Rising silver resistance documented	[166–170]
CuO	16–512	3–6	20–60	50–80	None	Low	Limited	Moderate	[171,172]
Au NPs	N/A (no intrinsic activity)	N/A	>500	40–70	Plasmonic SPR	Very high	Limited topical clearance	N/A	[173–175]
TiO_2	64–1024 (UV); >1024 (dark)	2–5	100–300	50–75	Photo-catalytic	Low	Cleared as sunscreen	Low (UV-only)	[176,177]
CeO_2	typically >1024	1–3	>500	50–80	Redox cycling	Moderate	Limited	Low	[178–180]
MgO	64–1024	2–4	200–500	40–70	None	Low	Limited	Low	[181,182]

Ag NP exhibits the strongest raw antimicrobial potency with sub-microgram-per-millilitre MICs, conversely with significant cytotoxicity to keratinocytes and fibroblasts show poor regenerative profile [96,97,166–170]. CuO NP are inexpensive and broad-spectrum, but exhibit higher hepatic accumulation and oxidative-stress toxicity than ZnO [171,172,183]. Au NP exhibits excellent biocompatibility and serves as drug-delivery payloads but lack intrinsic antibacterial activity [173–175]. TiO_2 are powerful photocatalysts under UV activation but are less active in dark visibility conditions which limit their clinical use [98,99,176,177]. CeO_2 NPs exhibit redox-cycling (Ce^{3+}/Ce^{4+}) ROS-scavenging activity which is therapeutic and relevant for inflammation, but lacks potent intrinsic antimicrobial efficacy. The antimicrobial action is attributed primarily to surface-mediated oxidative stress via localised ROS generation at the particle-membrane interface and minimally to electrostatic membrane disruption rather than to alkaline-pH-driven killing. CeO_2 NPs in comparison to ZnO NP whose antimicrobial activity is driven by a combination of Zn^{2+} ion release, direct membrane damage and intracellular ROS generation, demonstrates markedly lower and more concentration-dependent antibacterial performance [181,182]. From Table 6, it can be observed that ZnO exhibit positive viabilities on five axes simultaneously, including the only positive entry on intrinsic sensing, which is derived from its coupled piezoelectric, photoconductive and defect-mediated photoluminescent responses [163–165]. The compared eight-axis benchmarking is visualised in Figure 8. Nonetheless, it is worth noting that the tabulated values are representative figures from cited primary studies. Readers are referred to interpret these values as indicative rather than standard head-to-head measurements.

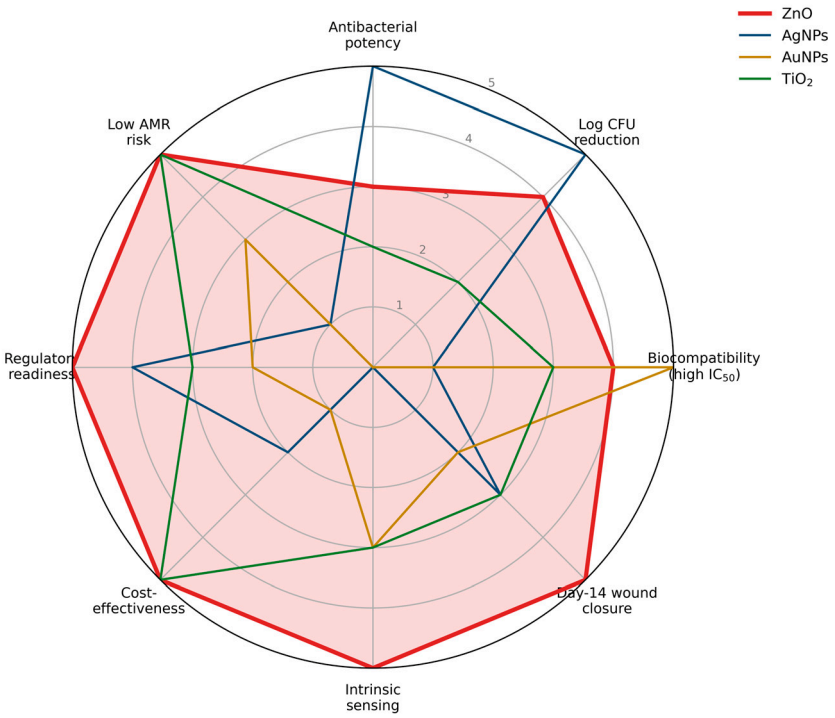

Figure 8. Eight-axis benchmarking of ZnO against representative metal and metal-oxide NPs.

The scores 1–5 in Figure 8 are used to qualitatively evaluate the tabulated evidence in Table 6 for burn wound care to demonstrate the combined antimicrobial–regenerative profile with intrinsic sensing capability of ZnO in comparison with metal and metal-oxide NPs.

4. Discussion

Existing works demonstrates the therapeutic performance of ZnO NP-based burn dressings is significantly affected by burn depth, infection burden, nanoparticle physicochemical properties and dressing architecture. In rodent partial- and full-thickness burn models, ZnO-containing hydrogels, nanofibers and polymeric films invariably improves wound contraction, re-epithelialisation, collagen deposition, and angiogenesis in comparison with untreated controls. Conversely, the magnitude of healing varies substantially across studies because of differences in NP size, concentration, surface chemistry and experimental methodology. ZnO NP exhibit broad-spectrum antibacterial activity against clinically relevant burn pathogens such as methicillin-resistant *Staphylococcus aureus* (MRSA), *Pseudomonas aeruginosa*, *Acinetobacter baumannii* and *Klebsiella pneumoniae*, primarily through combined mechanisms which involve ROS generation, membrane destabilisation and Zn^{2+} ion release. The antimicrobial and pro-regenerative effects of ZnO are mechanistically interconnected rather than independent. Controlled Zn^{2+} release contributes not only to bacterial growth inhibition and disruption of cellular homeostasis, other processes such as keratinocyte migration, fibroblast proliferation and Zn-dependent signalling pathways involved in tissue repair. Similarly, moderate ROS production can support antimicrobial activity and redox-mediated healing responses, whereas excessive ROS generation or rapid Zn^{2+} dissolution might induce mammalian cytotoxicity. This balance contributes to apparent discrepancy between the strong antimicrobial potency of sub-10 nm ZnO NP and the improved biocompatibility commonly reported for particles in the 20–50 nm range, where dissolution kinetics and oxidative stress are more controllable. Consequently, surface-modified or controlled-release ZnO systems are increasingly regarded as more clinically relevant formulations.

Future development of ZnO nanoparticle-based wound therapeutics is likely to focus on scalable manufacturing, data-driven materials optimisation, integrated theranostic systems, and improved translational models. Reproducibility challenges associated with biogenic ZnO synthesis may be addressed through continuous-flow microreactor platforms coupled with process analytical technologies including inline UV–Vis spectroscopy, dynamic light scattering and ICP-MS, enabling tighter control over nucleation kinetics, particle size distribution, surface chemistry, and Zn^{2+} release. Concurrently, machine-learning and active-learning approaches are powerful tools to navigate the multidimensional ZnO design space, including particle size, morphology, defect density, dopant chemistry and surface functionalisation to accelerate the optimisation of antimicrobial efficacy and biocompatibility. Additionally, the integration of ZnO nanomaterials into self-powered theranostic wound dressings represents a promising direction, especially through coupling PENGs, flexible biosensors, and low-power wireless communication modules for continuous monitoring of wound status without external power sources. Multi-analyte wearable sensing platforms capable of tracking pH, MMP-9, lactate, glucose, oxygen tension, and temperature may further enable personalised burn care strategies through real-time assessment of infection risk and healing progression. At the preclinical level, increasing adoption of organotypic human skin equivalents, skin-on-chip systems, and immune-competent organoid models is expected to improve translational relevance beyond conventional rodent wound models. Further, a broader clinical translation of ZnO NP wound technologies would require greater regulatory harmonisation such as standardised nanomaterial characterisation, toxicological evaluation and digital health validation frameworks aligned with key standards such as ISO 10993-1: 2025 and software-as-a-medical-device requirements [184].

5. Conclusions

ZnO NP is one of the few wound-care nanomaterials that combine broad-spectrum antimicrobial activity with pro-regenerative Zn^{2+} delivery and multi-functional physicochemical properties including piezoelectric, photo-responsive and pH-sensitive behaviour. Pre-clinical studies across hydrogel, nanofiber, and film-based burn dressings demonstrated improved wound contraction, re-epithelialisation, collagen deposition, and angiogenesis relative to untreated controls, together with strong antibacterial activity against clinically relevant burn pathogens. Existing works on antimicrobial efficacy is established to occur within the 3–7 log_10 CFU reduction range with minimum inhibitory concentrations, typically between 8 and 256 μg/mL. This phenomenon depending on the nanoparticle size, defect density, surface chemistry and testing conditions. The biological activity of ZnO arises from various interconnected mechanisms involving ROS generation, controlled Zn^{2+} ion release, membrane destabilisation, modulation of matrix metalloproteinases, especially MMP-2 and MMP-9, promotion of VEGF-associated angiogenesis and attenuation of excessive inflammatory signalling through partial suppression of NF-κB-mediated cytokine production. In parallel, the intrinsic piezoelectric and semiconducting properties of ZnO have enabled development of emerging theranostic wound dressings with capability to integrate biosensing, stimulus responsiveness and controlled therapeutic delivery within a single platform. Despite these advances, clinical translation is affected by several factors such as dose-dependent cytotoxicity associated with excessive ROS generation or Zn^{2+} dissolution, limited standardisation of green-synthesis methodologies, batch-to-batch variability in nanoparticle physicochemical properties and shortage of robust large-animal and clinical trial data. Progress toward clinical implementation will require harmonised characterisation standards encompassing particle size distribution, morphology, surface charge, defect density, dissolution kinetics, endotoxin burden, and ROS quantification, alongside scalable GMP-compatible manufacturing strategies such as continuous-flow synthesis. Future evaluation of sensor-integrated ZnO dressings in infected porcine burn models will provide a more clinically relevant bridge between current rodent studies and human burn care. In addition, the current work focussed on broad search across nano-bio and electrical engineering literature. The present review is limited by little under-representation of existing works on the subject patented and industry conference proceedings. However, the limitation is addressed with the rigorous literature search using key repositories including IEEE Xplore. Subsequently, future work will focus on patent searches to characterise the proprietary pipeline of ZnO for wound healing to elucidate the subject robustly.

Author Contributions: Conceptualisation, J.B.; methodology, J.B. and G.O.; validation, J.B., B.O., C.A. and G.O.; formal analysis, J.B. and G.O.; investigation, J.B., B.O., C.A. and G.O.; resources, J.B. and G.O.; data curation.; J.B., B.O. and C.A.; writing—original draft preparation, J.B., B.O. and C.A.; writing—review and editing, C.A. and G.O.; visualisation, J.B. and G.O.; supervision, G.O.; project administration, G.O. All authors have read and agreed to the published version of the manuscript.

Funding: This research received no external funding.

Institutional Review Board Statement: Not applicable.

Informed Consent Statement: Not applicable.

Data Availability Statement: No new data were created or analyzed in this study. Data sharing is not applicable to this article.

Acknowledgments: During the preparation of this manuscript, the authors used Biorender to design high-quality illustrative figures to elucidate the subject of the research. The authors have reviewed and edited the output and take full responsibility for the content of this publication.

Conflicts of Interest: The authors declare no conflict of interest.

Nomenclature

The following nomenclature are used in this manuscript:

Acronym/Symbol	Meaning
Ag	Silver
Au	Gold
GBD	Global Burden of Disease
NP	Nanoparticle
WHO	World Health Organisation
Ag NPs	Silver NP
Au NPs	Gold NP
BLE	Bluetooth Low Energy
CeO_2	Cerium Oxide
CFU	Colony-Forming Unit
CuO	Copper Oxide
CVD	Chemical Vapour Deposition
ECM	Extracellular Matrix
EPR	Electron Paramagnetic Resonance
EPS	Extracellular Polymeric Substances
GMP	Good Manufacturing Practice
HIF-1α	Hypoxia-Inducible Factor-1 Alpha
ICP-MS	Inductively Coupled Plasma Mass Spectrometry
IL-1β	Interleukin-1 Beta
IL-6	Interleukin-6
LoD	Limit of Detection
MgO	Magnesium Oxide
MIC	Minimum Inhibitory Concentration
MMP	Matrix Metalloproteinase
MRSA	Methicillin-Resistant Staphylococcus aureus
NFC	Near-Field Communication
NF-κB	Nuclear Factor Kappa B
NIR	Near-Infrared
PDMS	Polydimethylsiloxane
PENG	Piezoelectric Nanogenerator
PLGA	Poly(lactic-co-glycolic acid)
PVA	Polyvinyl Alcohol
ROS	Reactive Oxygen Species
SAW	Surface Acoustic Wave
TBSA	Total Body Surface Area
TiO2	Titanium Dioxide
TNF-α	Tumour Necrosis Factor Alpha
TPU	Thermoplastic Polyurethane
UV	Ultraviolet
VEGF	Vascular Endothelial Growth Factor
ZnO	Zinc Oxide

References

1. Madaghiele, M.; Demitri, C.; Sannino, A.; Ambrosio, L. Polymeric hydrogels for burn wound care: Advanced skin wound dressings and regenerative templates. *Burn. Trauma* **2014**, *2*, 153–161. [CrossRef] [PubMed]
2. Żwierełło, W.; Piorun, K.; Skórka-Majewicz, M.; Maruszewska, A.; Antoniewski, J.; Gutowska, I. Burns: Classification, Pathophysiology, and Treatment: A Review. *Int. J. Mol. Sci.* **2023**, *24*, 3749. [CrossRef] [PubMed]
3. Balaure, P.C.; Holban, A.M.; Grumezescu, A.M.; Mogoşanu, G.D.; Bălşeanu, T.A.; Stan, M.S.; Dinischiotu, A.; Volceanov, A.; Mogoantă, L. In vitro and in vivo studies of novel fabricated bioactive dressings based on collagen and zinc oxide 3D scaffolds. *Int. J. Pharm.* **2019**, *557*, 199–207. [CrossRef] [PubMed]

4. Stokes, M.A.R.; Johnson, W.D. Burns in the Third World: An unmet need. *Ann. Burn. Fire Disasters* **2017**, *30*, 243–246.
5. Radzikowska-Büchner, E.; Łopuszyńska, I.; Flieger, W.; Tobiasz, M.; Maciejewski, R.; Flieger, J. An Overview of Recent Developments in the Management of Burn Injuries. *Int. J. Mol. Sci.* **2023**, *24*, 16357. [CrossRef] [PubMed]
6. Bozkaya, O.; Bozkaya, E.; Ekici, H.; Alçığır, M.E.; Şahin, Y.; Çerçi, N.A.; Karahan, S.; Yiğitoğlu, M.; Vargel, I. Evaluation of Burn Wound Healing Efficacy and Biocompatibility of Centella asiatica Mediated Synthesised AgNPs Loaded Hybrid Nanofiber Scaffold: In Vitro and In Vivo Studies. *Macromol. Mater. Eng.* **2024**, *309*, 2400186. [CrossRef]
7. Souto, E.B.; Ribeiro, A.F.; Ferreira, M.I.; Teixeira, M.C.; Shimojo, A.A.M.; Soriano, J.L.; Naveros, B.C.; Durazzo, A.; Lucarini, M.; Souto, S.B.; et al. New Nanotechnologies for the Treatment and Repair of Skin Burns Infections. *Int. J. Mol. Sci.* **2020**, *21*, 393. [CrossRef] [PubMed]
8. Lee, N.; Bae, Y.; Jang, S.; Lee, D.W.; Lee, S.W. Global, Regional, and National Burden of Burn Injury by Total Body Surface Area (TBSA) Involvement from 1990 to 2021, with Projections of Prevalence to 2050. *Healthcare* **2025**, *13*, 2077. [CrossRef] [PubMed]
9. Tienda-Vázquez, M.A.; Hanel, J.M.; Márquez-Arteaga, E.M.; Salgado-Álvarez, A.P.; Scheckhuber, C.Q.; Alanis-Gómez, J.R.; Espinoza-Silva, J.I.; Ramos-Kuri, M.; Hernández-Rosas, F.; Melchor-Martínez, E.M.; et al. Exosomes: A Promising Strategy for Repair, Regeneration and Treatment of Skin Disorders. *Cells* **2023**, *12*, 1625. [CrossRef] [PubMed]
10. Nasra, S.; Pramanik, S.; Oza, V.; Kansara, K.; Kumar, A. Advancements in wound management: Integrating nanotechnology and smart materials for enhanced therapeutic interventions. *Discov. Nano* **2024**, *19*, 159. [CrossRef] [PubMed]
11. Jackson, D.M. The diagnosis of the depth of burning. *Br. J. Surg.* **1953**, *40*, 588–596. [CrossRef] [PubMed]
12. Siu, W.S.; Ma, H.; Leung, P.C. Review on Current Advancements in Facilitation of Burn Wound Healing. *Bioengineering* **2025**, *12*, 428. [CrossRef] [PubMed]
13. Kolimi, P.; Narala, S.; Nyavanandi, D.; Youssef, A.A.A.; Dudhipala, N. Innovative Treatment Strategies to Accelerate Wound Healing: Trajectory and Recent Advancements. *Cells* **2022**, *11*, 2439. [CrossRef] [PubMed]
14. Tipton, C.D.; Mathew, M.E.; Wolcott, R.A.; Wolcott, R.D.; Kingston, T.; Phillips, C.D. Temporal dynamics of relative abundances and bacterial succession in chronic wound communities. *Wound Repair Regen.* **2017**, *25*, 673–679. [CrossRef] [PubMed]
15. Shree, P.; Singh, C.K.; Sodhi, K.K.; Surya, J.N.; Singh, D.K. Biofilms: Understanding the structure and contribution towards bacterial resistance in antibiotics. *Med. Microecol.* **2023**, *16*, 100084. [CrossRef]
16. Haney, E.F.; Trimble, M.J.; Cheng, J.T.; Vallé, Q.; Hancock, R.E.W. Critical Assessment of Methods to Quantify Biofilm Growth and Evaluate Antibiofilm Activity of Host Defence Peptides. *Biomolecules* **2018**, *8*, 29. [CrossRef] [PubMed]
17. Kaya, M.; Akdaşçi, E.; Eker, F.; Bechelany, M.; Karav, S. Recent Advances of Silver Nanoparticles in Wound Healing: Evaluation of In Vivo and In Vitro Studies. *Int. J. Mol. Sci.* **2025**, *26*, 9889. [CrossRef] [PubMed]
18. Ortega-Llamas, L.; Quiñones-Vico, M.I.; García-Valdivia, M.; Fernández-González, A.; Ubago-Rodríguez, A.; la Torre, R.S.-D.; Arias-Santiago, S. Cytotoxicity and Wound Closure Evaluation in Skin Cell Lines after Treatment with Common Antiseptics for Clinical Use. *Cells* **2022**, *11*, 1395. [CrossRef] [PubMed]
19. Hosny, A.E.M.; Rasmy, S.A.; Aboul-Magd, D.S.; Kashef, M.T.; El-Bazza, Z.E. The increasing threat of silver-resistance in clinical isolates from wounds and burns. *Infect. Drug Resist.* **2019**, *12*, 1985–2001. [CrossRef] [PubMed]
20. Cretu, A.; Grosu-Bularda, A.; Bordeanu-Diaconescu, E.-M.; Hodea, F.-V.; Ratoiu, V.-A.; Dumitru, C.-S.; Andrei, M.-C.; Neagu, T.-P.; Lascar, I.; Hariga, C.-S. Strategies for Optimizing Acute Burn Wound Therapy: A Comprehensive Review. *Medicina* **2025**, *61*, 128. [CrossRef] [PubMed]
21. Yusuf, A.; Almotairy, A.R.Z.; Henidi, H.; Alshehri, O.Y.; Aldughaim, M.S. Nanoparticles as Drug Delivery Systems: A Review of the Implication of Nanoparticles' Physicochemical Properties on Responses in Biological Systems. *Polymers* **2023**, *15*, 1596. [CrossRef] [PubMed]
22. Joseph, T.M.; Mahapatra, D.K.; Esmaeili, A.; Piszczyk, Ł.; Hasanin, M.S.; Kattali, M.; Haponiuk, J.; Thomas, S. Nanoparticles: Taking a Unique Position in Medicine. *Nanomaterials* **2023**, *13*, 574. [CrossRef] [PubMed]
23. Loo, H.L.; Goh, B.H.; Lee, L.-H.; Chuah, L.H. Application of chitosan-based nanoparticles in skin wound healing. *Asian J. Pharm. Sci.* **2022**, *17*, 299–332. [CrossRef] [PubMed]
24. Mousavi, S.M.; Behbudi, G.; Gholami, A.; Hashemi, S.A.; Nejad, Z.M.; Bahrani, S.; Chiang, W.-H.; Wei, L.C.; Omidifar, N. Shape-controlled synthesis of zinc nanostructures mediating macromolecules for biomedical applications. *Biomater. Res.* **2022**, *26*, 4. [CrossRef] [PubMed]
25. Xiao, D.; Huang, Y.; Fang, Z.; Liu, D.; Wang, Q.; Xu, Y.; Li, P.; Li, J. Zinc oxide nanoparticles for skin wound healing: A systematic review from the perspective of disease types. *Mater. Today Bio* **2025**, *34*, 102221. [CrossRef] [PubMed]
26. Burlec, A.F.; Corciova, A.; Boev, M.; Batir-Marin, D.; Mircea, C.; Cioanca, O.; Danila, G.; Danila, M.; Bucur, A.F.; Hancianu, M. Current Overview of Metal Nanoparticles' Synthesis, Characterization, and Biomedical Applications, with a Focus on Silver and Gold Nanoparticles. *Pharmaceuticals* **2023**, *16*, 1410. [CrossRef] [PubMed]
27. Krithiga, N.; Rajalakshmi, A.; Jayachitra, A.; Khlebtsov, N. Green Synthesis of Silver Nanoparticles Using Leaf Extracts of Clitoria ternatea and Solanum nigrum and Study of Its Antibacterial Effect against Common Nosocomial Pathogens. *J. Nanosci.* **2015**, *2015*, 928204. [CrossRef]

28. Pormohammad, A.; Monych, N.K.; Ghosh, S.; Turner, D.L.; Turner, R.J. Nanomaterials in Wound Healing and Infection Control. *Antibiotics* **2021**, *10*, 473. [CrossRef] [PubMed]
29. Mendes, C.; Thirupathi, A.; Corrêa, M.; Gu, Y.; Silveira, P.C.L. The Use of Metallic Nanoparticles in Wound Healing: New Perspectives. *Int. J. Mol. Sci.* **2022**, *23*, 15376. [CrossRef] [PubMed]
30. Shaikh, S.; Nazam, N.; Rizvi, S.M.D.; Ahmad, K.; Baig, M.H.; Lee, E.J.; Choi, I. Mechanistic Insights into the Antimicrobial Actions of Metallic Nanoparticles and Their Implications for Multidrug Resistance. *Int. J. Mol. Sci.* **2019**, *20*, 2468. [CrossRef] [PubMed]
31. Medic, B.S.; Tomic, N.; Lagopati, N.; Gazouli, M.; Pojskic, L. Advances in Metal and Metal Oxide Nanomaterials for Topical Antimicrobial Applications: Insights and Future Perspectives. *Molecules* **2024**, *29*, 5551. [CrossRef] [PubMed]
32. Huq, M.A.; Apu, M.A.I.; Ashrafudoulla, M.; Rahman, M.M.; Parvez, M.A.K.; Balusamy, S.R.; Akter, S.; Rahman, M.S. Bioactive ZnO Nanoparticles: Biosynthesis, Characterization and Potential Antimicrobial Applications. *Pharmaceutics* **2023**, *15*, 2634. [CrossRef] [PubMed]
33. Luque-Morales, P.A.; Lopez-Peraza, A.; Nava-Olivas, O.J.; Amaya-Parra, G.; Baez-Lopez, Y.A.; Orozco-Carmona, V.M.; Garrafa-Galvez, H.E.; Chinchillas-Chinchillas, M.d.J. ZnO Semiconductor Nanoparticles and Their Application in Photocatalytic Degradation of Various Organic Dyes. *Materials* **2021**, *14*, 7537. [CrossRef] [PubMed]
34. Fulindi, R.B.; Barbosa, T.W.L.; Enriquez, V.; Charles-Niño, C.L.; de Freitas, N.G.; Salto, M.P.; Chiavacci, L.A.; Pratavieira, S.; Junior, J.P.A.; da Costa, P.I.; et al. Zinc-Based Nanoparticles Reduce the Bacterial Burden and Protect Collagen in a Mouse Cutaneous Wound Model. *ACS Omega* **2026**, *11*, 7115–7128. [CrossRef] [PubMed]
35. Jiang, S.; Lin, K.; Cai, M. ZnO Nanomaterials: Current Advancements in Antibacterial Mechanisms and Applications. *Front. Chem.* **2020**, *8*, 580. [CrossRef] [PubMed]
36. Shi, S.; Ou, X.; Long, J.; Lu, X.; Xu, S.; Zhang, L. Nanoparticle-Based Therapeutics for Enhanced Burn Wound Healing: A Comprehensive Review. *Int. J. Nanomed.* **2024**, *19*, 11213–11233. [CrossRef] [PubMed]
37. Huang, R.; Hu, J.; Qian, W.; Chen, L.; Zhang, D. Recent advances in nanotherapeutics for the treatment of burn wounds. *Burn. Trauma* **2021**, *9*, tkab026. [CrossRef] [PubMed]
38. Jeschke, M.G.; van Baar, M.E.; Choudhry, M.A.; Chung, K.K.; Gibran, N.S.; Logsetty, S. Burn injury. *Nat. Rev. Dis. Primers* **2020**, *6*, 11. [CrossRef] [PubMed]
39. Yang, M.I.; Girsang, E.; Nasution, A.N.; Ginting, C.N. Wound Healing Activity of Avocado Peel Ointment against Second Degree Burn Wound. In *Proceedings of the 2021 IEEE International Conference on Health, Instrumentation & Measurement, and Natural Sciences (InHeNce)*; IEEE: New York, NY, USA, 2021; pp. 1–6. [CrossRef]
40. Kolarijani, N.R.; Zamani, S.; Gharibshahian, M.; Aldaghi, N.; Semyari, H.; Vaez, A.; Rahmati, M.; Sohrabi, S.; Hedayat, F.; Gharravi, A.M.; et al. Accelerating burn wound healing using alginate/carboxymethyl cellulose nanogel containing *Tussilago farfara* and ZnO nanoparticle. *Burns* **2025**, *51*, 107700. [CrossRef] [PubMed]
41. Abarca-Pineda, Y.A.; Alaniz, I.C.; Ibraheam, A.; Bhasin, I.; Alasaadi, S.; Gracia, M.; Suresh, J.; Cai, L.Y.; Siddiqui, H.F.; García, M.L.; et al. Conventional and Emerging Surgical and Non-surgical Approaches to the Management of Skin Burn Scars: A Comprehensive Review. *Cureus* **2025**, *17*, e90982. [CrossRef] [PubMed]
42. Mofazzal Jahromi, M.A.; Zangabad, P.S.; Basri, S.M.M.; Zangabad, K.S.; Ghamarypour, A.; Aref, A.R.; Karimi, M.; Hamblin, M.R. Nanomedicine and advanced technologies for burns: Preventing infection and facilitating wound healing. *Adv. Drug Deliv. Rev.* **2018**, *123*, 33–64. [CrossRef] [PubMed]
43. Khatami, M.; Varma, R.S.; Zafarnia, N.; Yaghoobi, H.; Sarani, M.; Kumar, V.G. Applications of green synthesized Ag, ZnO and Ag/ZnO nanoparticles for making clinical antimicrobial wound-healing bandages. *Sustain. Chem. Pharm.* **2018**, *10*, 9–15. [CrossRef]
44. Doan Thi, T.U.; Nguyen, T.T.; Thi, Y.D.; Ta Thi, K.H.; Phan, B.T.; Pham, K.N. Green synthesis of ZnO nanoparticles using orange fruit peel extract for antibacterial activities. *RSC Adv.* **2020**, *10*, 23899–23907. [CrossRef] [PubMed]
45. Dey, S.; Mohanty, D.L.; Divya, N.; Bakshi, V.; Mohanty, A.; Rath, D.; Das, S.; Mondal, A.; Roy, S.; Sabui, R. A critical review on zinc oxide nanoparticles: Synthesis, properties and biomedical applications. *Intell. Pharm.* **2025**, *3*, 53–70. [CrossRef]
46. Hashemi, S.S.; Pakdin, A.; Mohammadi, A.; Keshavarzi, A.; Mortazavi, M.; Sanati, P. Study the Effect of Calendula officinalis Extract Loaded on Zinc Oxide Nanoparticle Cream in Burn Wound Healing. *ACS Appl. Mater. Interfaces* **2023**, *15*, 59269–59279. [CrossRef] [PubMed]
47. Ghaneialvar, H.; Soltani, L.; Mami, S.; Azizian, H.; Abbasi, N.; Gholami, M.; Molaei, S.; Ghadermazi, M.; Alizadeh, R.; Akbari, A.R.; et al. Green Synthesis of ZnO and Mg-doped ZnO Nanoparticles Using Ferulago angulata Plant Extract and Its Effect on Second-Degree Burn Wound Healing. *Cell Biochem. Funct.* **2025**, *43*, e70121. [CrossRef] [PubMed]
48. Alavi, M.; Nokhodchi, A. An overview on antimicrobial and wound healing properties of ZnO nanobiofilms, hydrogels, and bionanocomposites based on cellulose, chitosan, and alginate polymers. *Carbohydr. Polym.* **2020**, *227*, 115349. [CrossRef] [PubMed]
49. Yang, J.; Xiong, D.; Long, M. Zinc Oxide Nanoparticles as Next-Generation Feed Additives: Bridging Antimicrobial Efficacy, Growth Promotion, and Sustainable Strategies in Animal Nutrition. *Nanomaterials* **2025**, *15*, 1030. [CrossRef] [PubMed]

50. Lu, Z.; Gao, J.; He, Q.; Wu, J.; Liang, D.; Yang, H.; Chen, R. Enhanced antibacterial and wound healing activities of microporous chitosan-Ag/ZnO composite dressing. *Carbohydr. Polym.* **2017**, *156*, 460–469. [CrossRef] [PubMed]
51. Kang, H.; Buchman, J.T.; Rodriguez, R.S.; Ring, H.L.; He, J.; Bantz, K.C.; Haynes, C.L. Stabilization of Silver and Gold Nanoparticles: Preservation and Improvement of Plasmonic Functionalities. *Chem. Rev.* **2019**, *119*, 664–699. [CrossRef] [PubMed]
52. Hamdan, S.; Pastar, I.; Drakulich, S.; Dikici, E.; Tomic-Canic, M.; Deo, S.; Daunert, S. Nanotechnology-Driven Therapeutic Interventions in Wound Healing: Potential Uses and Applications. *ACS Cent. Sci.* **2017**, *3*, 163–175. [CrossRef] [PubMed]
53. Cortesi, R.; Sguizzato, M.; Ferrara, F. Lipid-based nanosystems for wound healing. *Expert Opin. Drug Deliv.* **2024**, *21*, 1191–1211. [CrossRef] [PubMed]
54. Sonje, D.P.; Chinchole, P.S.; Shende, P. Advancement in nanotechnology-based formulations for cell repairment in burns. *J. Drug Deliv. Sci. Technol.* **2025**, *111*, 107175. [CrossRef]
55. Zhai, M.; Xu, Y.; Zhou, B.; Jing, W. Keratin-chitosan/n-ZnO nanocomposite hydrogel for antimicrobial treatment of burn wound healing: Characterization and biomedical application. *J. Photochem. Photobiol. B* **2018**, *180*, 253–258. [CrossRef] [PubMed]
56. Sajjad, A.; Ali, H.; Zia, M. Fabrication and evaluation of vitamin doped Zno/AgNPs nanocomposite based wheat gluten films: A promising findings for burn wound treatment. *Sci. Rep.* **2023**, *13*, 16072. [CrossRef] [PubMed]
57. Beg, M.; Ghodinde, S.; Gupta, V. Plant mediated green synthesis of Zinc Oxide Nanoparticles for burn wound therapy. *Int. J. Adv. Res.* **2020**, *8*, 521–547. [CrossRef] [PubMed]
58. Shao, F.; Yang, A.; Yu, D.M.; Wang, J.; Gong, X.; Tian, H.X. Bio-synthesis of Barleria gibsoni leaf extract mediated zinc oxide nanoparticles and their formulation gel for wound therapy in nursing care of infants and children. *J. Photochem. Photobiol. B Biol.* **2018**, *189*, 267–273. [CrossRef] [PubMed]
59. Sudheesh Kumar, P.T.; Raj, N.M.; Praveen, G.; Chennazhi, K.P.; Nair, S.V.; Jayakumar, R. In vitro and in vivo evaluation of microporous chitosan hydrogel/nanofibrin composite bandage for skin tissue regeneration. *Tissue Eng. Part A* **2013**, *19*, 380–392. [CrossRef] [PubMed]
60. Kumar, H.K.N.; Mohana, N.C.; Nuthan, B.R.; Ramesha, K.P.; Rakshith, D.; Geetha, N.; Satish, S. Phyto-mediated synthesis of zinc oxide nanoparticles using aqueous plant extract of Ocimum americanum and evaluation of its bioactivity. *SN Appl. Sci.* **2019**, *1*, 651. [CrossRef]
61. Hong, L.; Zhou, N. Advancements in zinc oxide nanofibers for enhanced rehabilitation and injury recovery: Mechanisms, applications, and future directions. *J. Biol. Eng.* **2025**, *19*, 93. [CrossRef] [PubMed]
62. Lucian, B.I.; Cheregi, C.D.; Sebastian, H.M.; Ruxandra-Florina, B.; Maghiar, L.; Ilarie, B.; Anca, H.; Sachelarie, L.; Mircea-Ioan, S. Electrospun Nanofibers in Wound Healing: Real-World Evaluation of Spincare™ Technology. *Bioengineering* **2025**, *12*, 500. [CrossRef] [PubMed]
63. Goh, M.; Du, M.; Peng, W.R.; Saw, P.E.; Chen, Z. Advancing burn wound treatment: Exploring hydrogel as a transdermal drug delivery system. *Drug Deliv.* **2024**, *31*, 2300945. [CrossRef] [PubMed]
64. Yao, Y.; Zhang, A.; Yuan, C.; Chen, X.; Liu, Y. Recent trends on burn wound care: Hydrogel dressings and scaffolds. *Biomater. Sci.* **2021**, *9*, 4523–4540. [CrossRef] [PubMed]
65. You, T.; You, Q.; Feng, X.; Li, H.; Yi, B.; Xu, H. A novel approach to wound healing: Green synthetic nano-zinc oxide embedded with sodium alginate and polyvinyl alcohol hydrogels for dressings. *Int. J. Pharm.* **2024**, *654*, 123968. [CrossRef] [PubMed]
66. Patil, S.; Chandrasekaran, R. Biogenic nanoparticles: A comprehensive perspective in synthesis, characterization, application and its challenges. *J. Genet. Eng. Biotechnol. Rep.* **2020**, *18*, 67. [CrossRef] [PubMed]
67. Khan, N.; Arora, I.; Chandra, D.A.; Garg, S. Biofabrication of Nanoparticles in Wound-Healing Materials. In *Green Synthesis of Nanomaterials: Biological and Environmental Applications*; John Wiley & Sons, Inc.: Hoboken, NJ, USA, 2024; pp. 208–227.
68. Balaji, S.; Kumar, R.; Sripriya, R.; Kakkar, P.; Ramesh, D.V.; Reddy, P.N.K.; Sehgal, P. Preparation and comparative characterization of keratin–chitosan and keratin–gelatin composite scaffolds for tissue engineering applications. *Mater. Sci. Eng. C* **2012**, *32*, 975–982. [CrossRef]
69. Sirelkhatim, A.; Mahmud, S.; Seeni, A.; Kaus, N.H.M.; Ann, L.C.; Bakhori, S.K.M.; Hasan, H.; Mohamad, D. Review on Zinc Oxide Nanoparticles: Antibacterial Activity and Toxicity Mechanism. *Nano-Micro Lett.* **2015**, *7*, 219–242. [CrossRef] [PubMed]
70. Melnikova, N.; Balakireva, A.; Orekhov, D.; Kamorin, D.; Didenko, N.; Malygina, D.; Knyazev, A.; Novopoltsev, D.; Solovyeva, A. Zinc Oxide Nanoparticles Protected with Terpenoids as a Substance in Redox Imbalance Normalization in Burns. *Pharmaceuticals* **2021**, *14*, 492. [CrossRef] [PubMed]
71. Holmes, A.M.; Song, Z.; Moghimi, H.R.; Roberts, M.S. Relative Penetration of Zinc Oxide and Zinc Ions into Human Skin after Application of Different Zinc Oxide Formulations. *ACS Nano* **2016**, *10*, 1810–1819. [CrossRef] [PubMed]
72. Kavitha, S.; Dhamodaran, M.; Prasad, R.; Ganesan, M. Synthesis and characterisation of zinc oxide nanoparticles using terpenoid fractions of Andrographis paniculata leaves. *Int. Nano Lett.* **2017**, *7*, 141–147. [CrossRef]
73. Melnikova, N.; Vorobyova, O.; Balakireva, A.; Malygina, D.; Solovyeva, A.; Belyaeva, K.; Orekhov, D.; Knyazev, A. The New Pharmaceutical Compositions of Zinc Oxide Nanoparticles and Triterpenoids for the Burn Treatment. *Pharmaceuticals* **2020**, *13*, 207. [CrossRef] [PubMed]

74. Athamneh, T.; Abuawad, A.; Odat, T.; Alshweiat, A.; Obaidat, R.; Yaseen, F.B.; Al-Najjar, M.A.; Garafat, R.; Altarabeen, R.; Smirnova, I.; et al. Investigation of the Antibacterial Activity of ZnO-Loaded Alginate/Hyaluronic Acid Aerogels for Wound Dressing Applications. *Polymers* **2025**, *17*, 506. [CrossRef] [PubMed]
75. Sajjad, A.; Bhatti, S.H.; Ali, Z.; Jaffari, G.H.; Khan, N.A.; Rizvi, Z.F.; Zia, M. Photoinduced Fabrication of Zinc Oxide Nanoparticles: Transformation of Morphological and Biological Response on Light Irradiance. *ACS Omega* **2021**, *6*, 11783–11793. [CrossRef] [PubMed]
76. Sajjad, A.; Zia, M.; Xiao, X.; Olsson, R.; Capezza, A.J.; Rasheed, F. Wheat gluten hydrolysates with embedded Ag-nanoparticle; a structure-function assessment for potential applications as wound sorbents with antimicrobial properties. *Polym. Test.* **2022**, *118*, 107896. [CrossRef]
77. Nagaiah, H.P.; Samsudeen, M.B.; Augustus, A.R.; Shunmugiah, K.P. In vitro evaluation of silver-zinc oxide-eugenol nanocomposite for enhanced antimicrobial and wound healing applications in diabetic conditions. *Discov. Nano* **2025**, *20*, 14. [CrossRef] [PubMed]
78. Rakhshaei, R.; Namazi, H. A potential bioactive wound dressing based on carboxymethyl cellulose/ZnO impregnated MCM-41 nanocomposite hydrogel. *Mater. Sci. Eng. C Mater. Biol. Appl.* **2017**, *73*, 456–464. [CrossRef] [PubMed]
79. Pino, P.; Bosco, F.; Mollea, C.; Onida, B. Antimicrobial Nano-Zinc Oxide Biocomposites for Wound Healing Applications: A Review. *Pharmaceutics* **2023**, *15*, 970. [CrossRef] [PubMed]
80. Rajabloo, Z.; Farahpour, M.R.; Saffarian, P.; Jafarirad, S. Biofabrication of ZnO/Malachite nanocomposite and its coating with chitosan to heal infectious wounds. *Sci. Rep.* **2022**, *12*, 11592. [CrossRef] [PubMed]
81. Koumentakou, I.; Adamantidi, T.; Finos, M.A.; Efthymiopoulos, P.; Kosheleva, R.; Tsamesidis, I.; Kontonasaki, E.; Kyzas, G.Z. Chitosan-Based Nanocomposite Dressings Loaded with Zinc Oxide and Camphor for Hemostatic Applications. *Processes* **2026**, *14*, 1470. [CrossRef]
82. Liu, J.; Ismail, N.A.; Yusoff, M.; Razali, M.H.; Peana, M.F. Physicochemical Properties and Antibacterial Activity of Gellan Gum Incorporating Zinc Oxide/Carbon Nanotubes Bionanocomposite Film for Wound Healing. *Bioinorg. Chem. Appl.* **2022**, *2022*, 3158404. [CrossRef] [PubMed]
83. Hassen, A.; Moawed, E.A.; Bahy, R.; El Basaty, A.B.; El-Sayed, S.; Ali, A.I.; Tayel, A. Synergistic effects of thermally reduced graphene oxide/zinc oxide composite material on microbial infection for wound healing applications. *Sci. Rep.* **2024**, *14*, 22942. [CrossRef] [PubMed]
84. Jesline, A.; John, N.P.; Narayanan, P.M.; Vani, C.; Murugan, S. Antimicrobial activity of zinc and titanium dioxide nanoparticles against biofilm-producing methicillin-resistant Staphylococcus aureus. *Appl. Nanosci.* **2015**, *5*, 157–162. [CrossRef]
85. Hao, Y.; Wang, Y.; Zhang, L.; Liu, F.; Jin, Y.; Long, J.; Chen, S.; Duan, G.; Yang, H. Advances in antibacterial activity of zinc oxide nanoparticles against *Staphylococcus aureus* (Review). *BioMed Rep.* **2024**, *21*, 161. [CrossRef] [PubMed]
86. Abbas, Z.; Abdullah, H.; Hallaji, Z.; Ranjbar, B. Antibacterial and Antibiofilm Activity of Zinc Oxide Quantum Dots against Methicillin-resistant Staphylococcus aureus. *Part. Part Syst. Charact.* **2024**, *41*, 2400048. [CrossRef]
87. Kadiyala, U.; Turali-Emre, E.S.; Bahng, J.H.; Kotov, N.A.; VanEpps, J.S. Unexpected insights into antibacterial activity of zinc oxide nanoparticles against methicillin resistant *Staphylococcus aureus* (MRSA). *Nanoscale* **2018**, *10*, 4927–4939. [CrossRef] [PubMed]
88. Hassan, A.; Al-Salmi, F.A.; Saleh, M.A.; Sabatier, J.-M.; Alatawi, F.A.; Alenezi, M.A.; Albalwe, F.M.; Albalawi, H.M.R.; Darwish, D.B.E.; Sharaf, E.M. Inhibition Mechanism of Methicillin-Resistant *Staphylococcus aureus* by Zinc Oxide Nanorods via Suppresses Penicillin-Binding Protein 2a. *ACS Omega* **2023**, *8*, 9969–9977. [CrossRef] [PubMed]
89. Sheferov, I.; Balakireva, A.; Panteleev, D.; Spitskaya, I.; Orekhov, S.; Kazantsev, O.; Solovyeva, A.; Novopoltsev, D.; Melnikova, N. The Effect of Zinc Oxide Nanoparticles on Properties and Burn Wound Healing Activity of Thixotropic Xymedone Gels. *Sci. Pharm.* **2022**, *90*, 61. [CrossRef]
90. Krishnamoorthy, U.; Ramjan Begam, A.; Keerthiga, S.; Sakthi Kathir, M.; Selvaharini, S.; Vadivelan, S.S. Exploring multi-component nanofiber architectures of ZnO, curcumin, and andrographis paniculata for advanced wound care applications. *Next Nanotechnol.* **2026**, *9*, 100362. [CrossRef]
91. Blinov, A.V.; Kachanov, M.D.; Gvozdenko, A.A.; Nagdalian, A.A.; Blinova, A.A.; Rekhman, Z.A.; Golik, A.B.; Vakalov, D.S.; Maglakelidze, D.G.; Nagapetova, A.G.; et al. Synthesis and Characterization of Zinc Oxide Nanoparticles Stabilized with Biopolymers for Application in Wound-Healing Mixed Gels. *Gels* **2023**, *9*, 57. [CrossRef] [PubMed]
92. Sheferov, I.A.; Emasheva, A.A.; Sheferova, A.A.; Panteleev, D.A.; Mitin, A.V.; Kuzmichev, V.V.; Melnikova, N.B. Study of xymedone release from hydrogels with zinc oxide nanoparticles. *J. Drug Deliv. Ther.* **2024**, *14*, 43–48. [CrossRef]
93. Mejjo, D.B.; Nayal, R.; Abdelwahed, W.; Abajy, M.Y. Anti-Arthritis and Biosafety Properties of Green Synthesized Zinc Oxide Nanoparticles Loaded with Cedrus libani Extract. *Int. J. Nanomed.* **2025**, *20*, 11525–11551. [CrossRef] [PubMed]
94. Bhutto, A.A.; Kadhem, A.A.; Nawaz, L.; Haider, K.; Gupta, A. Nanoparticle-driven wound healing: Exploring the antioxidant and antibacterial potential of ZnO-based therapeutics. *J. Med. Health Sci. Rev.* **2025**, *2*, 5519–5531. [CrossRef]
95. El Turk, S.; Chekkaramkodi, D.; Ram, A.; Soliman, A.; Schiffer, A.; Zheng, L.; Butt, H. Role of metal nanomaterials in wound healing—A review. *Front. Bioeng. Biotechnol.* **2025**, *13*, 1665218. [CrossRef] [PubMed]

96. Ravikumar, S.; Velappan, K.; Munusamy, S.; Varnika, M.; Naveenaa, S.; Shanmugam, R. Emerging nanotechnologies in wound care: The role of metal and polymeric nanocomposites in enhancing healing and combating infections. *Int. J. Pharm.* **2025**, *684*, 126143. [CrossRef] [PubMed]
97. Wang, W.; Lu, K.J.; Yu, C.H.; Huang, Q.L.; Du, Y.Z. Nano-drug delivery systems in wound treatment and skin regeneration. *J. Nanobiotechnology* **2019**, *17*, 82. [CrossRef] [PubMed]
98. Annu; Bhat, Z.I.; Imtiyaz, K.; Rizvi, M.M.A.; Ikram, S.; Shin, D.K. Comparative Study of ZnO-and-TiO_2-Nanoparticles-Functionalized Polyvinyl Alcohol/Chitosan Bionanocomposites for Multifunctional Biomedical Applications. *Polymers* **2023**, *15*, 3477. [CrossRef] [PubMed]
99. Xie, J.; Li, H.; Zhang, T.; Song, B.; Wang, X.; Gu, Z. Recent Advances in ZnO Nanomaterial-Mediated Biological Applications and Action Mechanisms. *Nanomaterials* **2023**, *13*, 1500. [CrossRef] [PubMed]
100. Valadi, M.; Doostan, M.; Khoshnevisan, K.; Maleki, H. Enhanced healing of burn wounds by multifunctional alginate-chitosan hydrogel enclosing silymarin and zinc oxide nanoparticles. *Burns* **2024**, *50*, 2029–2044. [CrossRef] [PubMed]
101. Kołodziejczak-Radzimska, A.; Jesionowski, T. Zinc Oxide-From Synthesis to Application: A Review. *Materials* **2014**, *7*, 2833–2881. [CrossRef] [PubMed]
102. Mandal, A.K.; Katuwal, S.; Tettey, F.; Gupta, A.; Bhattarai, S.; Jaisi, S.; Bhandari, D.P.; Shah, A.K.; Bhattarai, N.; Parajuli, N. Current Research on Zinc Oxide Nanoparticles: Synthesis, Characterization, and Biomedical Applications. *Nanomaterials* **2022**, *12*, 3066. [CrossRef] [PubMed]
103. Varsha, A.; Bharathraj, A.; Shivanee, K.; Sahana, R.K.; Babu, S.; Selvamurugan, N. Unveiling the potential of inorganic nanoparticle-based scaffolds in wound healing: Advances in antimicrobial and regenerative strategies. *Nanoscale Adv.* **2026**, *8*, 395–421. [CrossRef] [PubMed]
104. Khorsandi, K.; Hosseinzadeh, R.; Esfahani, H.; Zandsalimi, K.; Shahidi, F.K.; Abrahamse, H. Accelerating skin regeneration and wound healing by controlled ROS from photodynamic treatment. *Inflamm. Regen.* **2022**, *42*, 40. [CrossRef] [PubMed]
105. Hamedi, S.; Shojaosadati, S.A. Preparation of antibacterial ZnO NP-containing schizophyllan/bacterial cellulose nanocomposite for wound dressing. *Cellulose* **2021**, *28*, 9269–9282. [CrossRef]
106. Khan, A.U.R.; Huang, K.; Jinzhong, Z.; Zhu, T.; Morsi, Y.; Aldalbahi, A.; El-Newehy, M.; Yan, X.; Mo, X. Exploration of the antibacterial and wound healing potential of a PLGA/silk fibroin based electrospun membrane loaded with zinc oxide nanoparticles. *J. Mater. Chem. B* **2021**, *9*, 1452–1465. [CrossRef] [PubMed]
107. Sharifi, S.; Hajipour, M.J.; Gould, L.; Mahmoudi, M. Nanomedicine in Healing Chronic Wounds: Opportunities and Challenges. *Mol. Pharm.* **2021**, *18*, 550–575. [CrossRef] [PubMed]
108. Pati, R.; Mehta, R.K.; Mohanty, S.; Padhi, A.; Sengupta, M.; Vaseeharan, B.; Goswami, C.; Sonawane, A. Topical application of zinc oxide nanoparticles reduces bacterial skin infection in mice and exhibits antibacterial activity by inducing oxidative stress response and cell membrane disintegration in macrophages. *Nanomed. Nanotechnol. Biol. Med.* **2014**, *10*, 1195–1208. [CrossRef] [PubMed]
109. Kushwaha, A.; Goswami, L.; Kim, B.S. Nanomaterial-Based Therapy for Wound Healing. *Nanomaterials* **2022**, *12*, 618. [CrossRef] [PubMed]
110. Shahzadi, L.; Chaudhry, A.A.; Aleem, A.R.; Malik, M.H.; Ijaz, K.; Akhtar, H.; Alvi, F.; Khan, A.F.; Rehman, I.U.; Yar, M. Development of K-doped ZnO nanoparticles encapsulated crosslinked chitosan based new membranes to stimulate angiogenesis in tissue engineered skin grafts. *Int. J. Biol. Macromol.* **2018**, *120*, 721–728. [CrossRef] [PubMed]
111. Yang, G.; Zhang, M.; Qi, B.; Zhu, Z.; Yao, J.; Yuan, X.; Sun, D. Nanoparticle-Based Strategies and Approaches for the Treatment of Chronic Wounds. *J. Biomater. Tissue Eng.* **2018**, *8*, 455–464. [CrossRef]
112. Raguvaran, R.; Manuja, B.K.; Chopra, M.; Thakur, R.; Anand, T.; Kalia, A.; Manuja, A. Sodium alginate and gum acacia hydrogels of ZnO nanoparticles show wound healing effect on fibroblast cells. *Int. J. Biol. Macromol.* **2017**, *96*, 185–191. [CrossRef] [PubMed]
113. Rayyif, S.M.I.; Mohammed, H.B.; Curuțiu, C.; Bîrcă, A.C.; Grumezescu, A.M.; Vasile, B.Ș.; Dițu, L.M.; Lazăr, V.; Chifiriuc, M.C.; Mihăescu, G.; et al. ZnO Nanoparticles-Modified Dressings to Inhibit Wound Pathogens. *Materials* **2021**, *14*, 3084. [CrossRef] [PubMed]
114. Karahaliloglu, Z.; Kilicay, E.; Denkbas, E.B. Antibacterial chitosan/silk sericin 3D porous scaffolds as a wound dressing material. *Artif. Cells Nanomed. Biotechnol.* **2017**, *45*, 1172–1185. [CrossRef] [PubMed]
115. Soubhagya, A.S.; Moorthi, A.; Prabaharan, M. Preparation and characterization of chitosan/pectin/ZnO porous films for wound healing. *Int. J. Biol. Macromol.* **2020**, *157*, 135–145. [CrossRef] [PubMed]
116. Aydin Acar, C.; Gencer, M.A.; Pehlivanoglu, S.; Yesilot, S.; Donmez, S. Green and eco-friendly biosynthesis of zinc oxide nanoparticles using Calendula officinalis flower extract: Wound healing potential and antioxidant activity. *Int. Wound J.* **2024**, *21*, e14413. [CrossRef] [PubMed]
117. Nandhini, J.; Karthikeyan, E.; Rajeshkumar, S. Green synthesis of zinc oxide nanoparticles: Eco-friendly advancements for biomedical marvels. *Resour. Chem. Mater.* **2024**, *3*, 294–316. [CrossRef]

118. Tosyalı, Ö.; Esentürk-Güzel, I.; İzBudak, B.; Abdo, L.; Bal-Öztürk, A.; Özkanca, C.; Döşler, S.; Karal-Yılmaz, O. Development of Chitosan and Silk Fibroin Nanofibers Incorporated With ZnO and TiO_2 Nanoparticles for Wound Dressing Applications. *J. Appl. Polym. Sci.* **2025**, *143*, e57941. [CrossRef]
119. Aly, A.A.; Ahmed, M.K. Nanofibers of cellulose acetate containing ZnO nanoparticles/graphene oxide for wound healing applications. *Int. J. Pharm.* **2021**, *598*, 120325. [CrossRef] [PubMed]
120. Safari, P.; Rahimabadi, E.Z.; Vaezi, M.R.; Behnamghader, A.; Tahergorabi, R. Development of ZnO-NPs reinforced chitosan nanofiber mats with improved antibacterial and biocompatibility properties. *Sci. Rep.* **2025**, *15*, 16567. [CrossRef] [PubMed]
121. Kalirajan, C.; Palanisamy, T. A ZnO-curcumin nanocomposite embedded hybrid collagen scaffold for effective scarless skin regeneration in acute burn injury. *J. Mater. Chem. B* **2019**, *7*, 5873–5886. [CrossRef] [PubMed]
122. Cleetus, C.M.; Primo, F.A.; Fregoso, G.; Raveendran, N.L.; Noveron, J.C.; Spencer, C.T.; Ramana, C.V.; Joddar, B. Alginate Hydrogels with Embedded ZnO Nanoparticles for Wound Healing Therapy. *Int. J. Nanomed.* **2020**, *15*, 5097–5111. [CrossRef] [PubMed]
123. Kurd, N.J.; Mirza, E.H.; Khan, T.; Rehman, M.A.U.; Rizwan, M.; Khan, A.A.; Alkhureif, A.A.; Vallittu, P.K. ZnO nanoparticles infused PVA-hyaluronic acid based hydrogel: An alternative solution for skin wound. *J. Mech. Behav. Biomed. Mater.* **2026**, *175*, 107324. [CrossRef] [PubMed]
124. Selvaraj, S.; Subbarayan, R.; Radhakrishnan, A.; Chauhan, A. Cellulose-Based Nanocomposites Loaded with Zinc Oxide Nanoparticles for Enhanced Wound Healing Applications. *ChemistrySelect* **2025**, *10*, e01622. [CrossRef]
125. Yaakob, M.; Hussin, N.H.; Kudin, T.I.T.; Hassan, O.; Ali, A.M.M.; Yahya, M.Z.A. First Principles LDA plus U Calculations for ZnO Materials. *Integr. Ferroelectr.* **2014**, *155*, 15–22. [CrossRef]
126. Verma, L.M.; Kumar, A.; Bashir, A.U.; Gangwar, U.; Ingole, P.P.; Sharma, S. Phase controlled green synthesis of wurtzite (P63mc) ZnO nanoparticles: Interplay of green ligands with precursor anions, anisotropy and photocatalysis. *Nanoscale Adv.* **2023**, *6*, 155–169. [CrossRef] [PubMed]
127. Zhang, X.; Huang, Y.; Wang, J.; Tang, J.; Mei, Y.; Zhu, N.; Li, Z.; Li, L.; Wang, Y. Facet-dependent transformation and toxicity of nanoscale zinc oxide in the synthetic saliva. *J. Environ. Sci.* **2024**, *139*, 170–181. [CrossRef] [PubMed]
128. Aicher, K.; Berger, T.; Aschauer, U.; Diwald, O. Ubiquitous shallow trap states and lattice hydrogenation of ZnO particles. *J. Mater. Chem. C Mater.* **2025**, *13*, 22625–22637. [CrossRef] [PubMed]
129. Barnasas, A.; Kanistras, N.; Ntagkas, A.; Anyfantis, D.; Stamatelatos, A.; Kapaklis, V.; Bouropoulos, N.; Mystiridou, E.; Poulopoulos, P.; Garoufalis, C.; et al. Quantum confinement effects of thin ZnO films by experiment and theory. *Phys. E Low-Dimens. Syst. Nanostruct.* **2020**, *120*, 114072. [CrossRef]
130. Chan, Y.B.; Aminuzzaman, M.; Chuah, X.-T.; Li, K.; Balu, P.; Wong, L.S.; Guha, S.K.; Tey, L.-H. Review in green synthesis mechanisms, application, and future prospects for *Garcinia mangostana* L. (mangosteen)-derived nanoparticles. *Nanotechnol. Rev.* **2025**, *14*, 20250157. [CrossRef]
131. Hao, N.; Zhang, M.; Zhang, J.X.J. Microfluidics for ZnO micro-/nanomaterials development: Rational design, controllable synthesis, and on-chip bioapplications. *Biomater. Sci.* **2020**, *8*, 1783–1801. [CrossRef] [PubMed]
132. Ben Amor, I.; Hemmami, H.; Laouini, S.E.; Mahboub, M.S.; Barhoum, A. Sol-Gel Synthesis of ZnO Nanoparticles Using Different Chitosan Sources: Effects on Antibacterial Activity and Photocatalytic Degradation of AZO Dye. *Catalysts* **2022**, *12*, 1611. [CrossRef]
133. Aalami, Z.; Hoseinzadeh, M.; Manesh, P.H.; Aalami, A.H.; Es'haghi, Z.; Darroudi, M.; Sahebkar, A.; Hosseini, H.A. Synthesis, characterization, and photocatalytic activities of green sol-gel ZnO nanoparticles using Abelmoschus esculentus and Salvia officinalis: A comparative study versus co-precipitation-synthesized nanoparticles. *Heliyon* **2024**, *10*, e24212. [CrossRef] [PubMed]
134. Anaya-Zavaleta, J.C.; Ledezma-Pérez, A.S.; Gallardo-Vega, C.; Rodríguez-Hernández, J.; Alvarado-Canché, C.N.; García-Casillas, P.E.; de León, A.; Herrera-May, A.L. ZnO Nanoparticles by Hydrothermal Method: Synthesis and Characterization. *Technologies* **2025**, *13*, 18. [CrossRef]
135. Wang, Y.; Yang, C.; Liu, Y.; Fan, Y.; Dang, F.; Qiu, Y.; Zhou, H.; Wang, W.; Liu, Y. Solvothermal Synthesis of ZnO Nanoparticles for Photocatalytic Degradation of Methyl Orange and p-Nitrophenol. *Water* **2021**, *13*, 3224. [CrossRef]
136. Saloga, P.E.J.; Thünemann, A.F. Microwave-Assisted Synthesis of Ultrasmall Zinc Oxide Nanoparticles. *Langmuir* **2019**, *35*, 12469–12482. [CrossRef] [PubMed]
137. Raghupathy, D.A.; Ramgopal, G.; Kumar, V.D.; Kumar, T.N.; Ravikumar, C. Study of Bi-functional Applications of ZnO Nanoparticles Synthesized via Sonochemical Route. *Asian J. Chem.* **2023**, *35*, 2929–2938. [CrossRef]
138. Wirunchit, S.; Gansa, P.; Koetniyom, W. Synthesis of ZnO nanoparticles by Ball-milling process for biological applications. *Mater. Today Proc.* **2021**, *47*, 3554–3559. [CrossRef]
139. Mintcheva, N.; Aljulaih, A.A.; Wunderlich, W.; Kulinich, S.A.; Iwamori, S. Laser-Ablated ZnO Nanoparticles and Their Photocatalytic Activity toward Organic Pollutants. *Materials* **2018**, *11*, 1127. [CrossRef] [PubMed]
140. Jin, S.E.; Jin, H.E. Synthesis, Characterization, and Three-Dimensional Structure Generation of Zinc Oxide-Based Nanomedicine for Biomedical Applications. *Pharmaceutics* **2019**, *11*, 575. [CrossRef] [PubMed]

141. Nandhini, J.; Karthikeyan, E.; Rajeshkumar, S. Nanomaterials for wound healing: Current status and futuristic frontier. *Biomed. Technol.* **2024**, *6*, 26–45. [CrossRef]
142. Wang, L.; Hu, C.; Shao, L. The antimicrobial activity of nanoparticles: Present situation and prospects for the future. *Int. J. Nanomed.* **2017**, *12*, 1227–1249. [CrossRef] [PubMed]
143. Baig, A.; Siddique, M.; Panchal, S. A Review of Visible-Light-Active Zinc Oxide Photocatalysts for Environmental Application. *Catalysts* **2025**, *15*, 100. [CrossRef]
144. Lu, L.; Zhao, Y.; Li, M.; Wang, X.; Zhu, J.; Liao, L.; Wang, J. Contemporary strategies and approaches for characterizing composition and enhancing biofilm penetration targeting bacterial extracellular polymeric substances. *J. Pharm. Anal.* **2024**, *14*, 100906. [CrossRef] [PubMed]
145. Carlos, G.O.; Neto, B.M.; Teixeira, L.F.S.; de Sousa, A.S.; Mathor, M.B.; Marumo, M.H.B. Zinc as a Dual-Condition Inhibitor of HIF-1α/VEGF-α-Mediated Angiogenesis in Clear Cell Renal Carcinoma. *J. Kidney Cancer VHL* **2025**, *12*, 35–45. [CrossRef] [PubMed]
146. Alqaffaf, D.; Atoom, A.M.; Abu Huwaij, R.; Abusalah, M.A.H.A.; Alzubi, B.T.; Al-Kaabneh, A.; Sughayer, M.A. Analysis of the antimicrobial activity of zinc oxide nanoparticles against drug-resistant bacteria and their applications in the disinfection process. *PLoS ONE* **2026**, *21*, e0340470. [CrossRef] [PubMed]
147. Ancona, A.; Dumontel, B.; Garino, N.; Demarco, B.; Chatzitheodoridou, D.; Fazzini, W.; Engelke, H.; Cauda, V. Lipid-Coated Zinc Oxide Nanoparticles as Innovative ROS-Generators for Photodynamic Therapy in Cancer Cells. *Nanomaterials* **2018**, *8*, 143. [CrossRef] [PubMed]
148. Riahi, S.; Ben Moussa, N.; Lajnef, M.; Jebari, N.; Dabek, A.; Chtourou, R.; Guisbiers, G.; Vimont, S.; Herth, E. Bactericidal activity of ZnO nanoparticles against multidrug-resistant bacteria. *J. Mol. Liq.* **2023**, *387*, 122596. [CrossRef]
149. Peng, H.; Rossetto, D.; Mansy, S.S.; Jordan, M.C.; Roos, K.P.; Chen, I.A. Treatment of Wound Infections in a Mouse Model Using Zn^{2+}-Releasing Phage Bound to Gold Nanorods. *ACS Nano* **2022**, *16*, 4756–4774. [CrossRef] [PubMed]
150. Ogawa, Y.; Kinoshita, M.; Shimada, S.; Kawamura, T. Zinc in Keratinocytes and Langerhans Cells: Relevance to the Epidermal Homeostasis. *J. Immunol. Res.* **2018**, *2018*, 5404093. [CrossRef] [PubMed]
151. Guo, D.D.; Li, Q.N.; Li, C.M.; Bi, H.S. Zinc oxide nanoparticles inhibit murine photoreceptor-derived cell proliferation and migration via reducing TGF-β and MMP-9 expression in vitro. *Cell Prolif.* **2015**, *48*, 198–208. [CrossRef] [PubMed]
152. Bhadwal, N.; Ben Mrad, R.; Behdinan, K. Review of Zinc Oxide Piezoelectric Nanogenerators: Piezoelectric Properties, Composite Structures and Power Output. *Sensors* **2023**, *23*, 3859. [CrossRef] [PubMed]
153. Rafati, F.; Johari, N.; Zhang, W. Synergistic triboelectric and piezoelectric effects in zinc oxide-based nanogenerators. *Micro Nanostruct.* **2026**, *210*, 208481. [CrossRef]
154. Nunez, C.G.; Vilouras, A.; Taube Navaraj, W.; Liu, F.; Dahiya, R. ZnO Nanowires-Based Flexible UV Photodetector System for Wearable Dosimetry. *IEEE Sens. J.* **2018**, *18*, 7881–7888. [CrossRef]
155. Liang, C.; Yan, C.; Zhai, S.; Wang, Y.; Hu, A.; Wang, W.; Pan, Y. Recent Progress in Flexible Surface Acoustic Wave Sensing Technologies. *Micromachines* **2024**, *15*, 357. [CrossRef] [PubMed]
156. Lv, J.; Li, C.; Chai, Z. Defect luminescence and its mediated physical properties in ZnO. *J. Lumin.* **2018**, *208*, 225–237. [CrossRef]
157. Aydoğdu, G.; Zeybek, D.K.; Pekyardımcı, Ş.; Kılıç, E. A novel amperometric biosensor based on ZnO nanoparticles-modified carbon paste electrode for determination of glucose in human serum. *Artif. Cells Nanomed. Biotechnol.* **2013**, *41*, 332–338. [CrossRef] [PubMed]
158. Castro, K.; Matias, R.; Cardoso, A.; Freitas, R.C.; de Oliveira, A.M.; Silva, T.A.; Janegitz, B.C. Exploring Lactate Electrochemical Biosensors: From Current Technologies to Future Market Impact. *Chemosensors* **2025**, *13*, 402. [CrossRef]
159. Chinnappan, R.; Ramachandran, L.; Uttam, I.; Citartan, M.; Ballal, N.V.; Mani, N.K. From Biomarkers to Biosensors: Modern Approaches for the Detection of Matrix Metalloproteinases (MMPs). *Biosensors* **2025**, *15*, 603. [CrossRef] [PubMed]
160. Jindal, K.; Gupta, V.; Tomar, M. Electrocatalytic Properties of ZnO Thin Film Based Biosensor for Detection of Uric Acid. In *Advanced Functional Materials and Devices: Select Proceedings of AFMD 2021*; Springer: Singapore, 2022; pp. 1–16.
161. Sun, X.; Guo, X.; Gao, J.; Wu, J.; Huang, F.; Zhang, J.-H.; Huang, F.; Lu, X.; Shi, Y.; Pan, L. E-Skin and Its Advanced Applications in Ubiquitous Health Monitoring. *Biomedicines* **2024**, *12*, 2307. [CrossRef] [PubMed]
162. Chen, X.; Xiong, H.; Chen, J.; Kong, J.; Zhang, Y.; Fang, X. Recent Progress in Wearable Bioelectronics for Theranostics and Perspectives with Artificial Intelligence. *ACS Appl. Mater. Interfaces* **2025**, *17*, 61604–61625. [CrossRef] [PubMed]
163. Raghupathi, K.R.; Koodali, R.T.; Manna, A.C. Size-dependent bacterial growth inhibition and mechanism of antibacterial activity of zinc oxide nanoparticles. *Langmuir* **2011**, *27*, 4020–4028. [CrossRef] [PubMed]
164. Baek, S.; Joo, S.H.; Kumar, N.; Toborek, M. Antibacterial effect and toxicity pathways of industrial and sunscreen ZnO nanoparticles on *Escherichia coli*. *J. Environ. Chem. Eng.* **2017**, *5*, 3024–3032. [CrossRef]
165. Wang, Z.L.; Song, J. Piezoelectric nanogenerators based on zinc oxide nanowire arrays. *Science* **2006**, *312*, 242–246. [CrossRef] [PubMed]

166. Panáček, A.; Kvítek, L.; Smékalová, M.; Večeřová, R.; Kolář, M.; Röderová, M.; Dyčka, F.; Šebela, M.; Prucek, R.; Tomanec, O.; et al. Bacterial resistance to silver nanoparticles and how to overcome it. *Nat. Nanotechnol.* **2018**, *13*, 65–71. [CrossRef] [PubMed]
167. Panáček, A.; Kvitek, L.; Prucek, R.; Kolar, M.; Vecerova, R.; Pizurova, N.; Sharma, V.K.; Nevecna, T.; Zboril, R. Silver colloid nanoparticles: Synthesis, characterization, and their antibacterial activity. *J. Phys. Chem. B* **2006**, *110*, 16248–16253. [CrossRef] [PubMed]
168. Martínez-Gutierrez, F.; Thi, E.P.; Silverman, J.M.; de Oliveira, C.C.; Svensson, S.L.; Vanden Hoek, A.; Sanchez, E.M.; Reiner, N.E.; Gaynor, E.C.; Pryzdial, E.L.G.; et al. Antibacterial activity, inflammatory response, coagulation and cytotoxicity effects of silver nanoparticles. *Nanomed. Nanotechnol. Biol. Med.* **2012**, *8*, 328–336. [CrossRef] [PubMed]
169. Galandáková, A.; Franková, J.; Ambrožová, N.; Habartová, K.; Pivodová, V.; Zálešák, B.; Šafářová, K.; Smékalová, M.; Ulrichová, J. Effects of silver nanoparticles on human dermal fibroblasts and epidermal keratinocytes. *Hum. Exp. Toxicol.* **2016**, *35*, 946–957. [CrossRef] [PubMed]
170. Bruna, T.; Maldonado-Bravo, F.; Jara, P.; Caro, N. Silver nanoparticles and their antibacterial applications. *Int. J. Mol. Sci.* **2021**, *22*, 7202. [CrossRef] [PubMed]
171. Karlsson, H.L.; Cronholm, P.; Gustafsson, J.; Möller, L. Copper oxide nanoparticles are highly toxic: A comparison between metal oxide nanoparticles and carbon nanotubes. *Chem. Res. Toxicol.* **2008**, *21*, 1726–1732. [CrossRef] [PubMed]
172. Gudkov, S.V.; Burmistrov, D.E.; Fomina, P.A.; Validov, S.Z.; Kozlov, V.A. Antibacterial properties of copper oxide nanoparticles (review). *Int. J. Mol. Sci.* **2024**, *25*, 11563. [CrossRef] [PubMed]
173. Dykman, L.; Khlebtsov, N. Gold nanoparticles in biomedical applications: Recent advances and perspectives. *Chem. Soc. Rev.* **2012**, *41*, 2256–2282. [CrossRef] [PubMed]
174. Zhou, Y.; Kong, Y.; Kundu, S.; Cirillo, J.D.; Liang, H. Antibacterial activities of gold and silver nanoparticles against Escherichia coli and bacillus Calmette-Guérin. *J. Nanobiotechnology* **2012**, *10*, 19. [CrossRef] [PubMed]
175. Unser, S.; Bruzas, I.; He, J.; Sagle, L. Localized surface plasmon resonance biosensing: Current challenges and approaches. *Sensors* **2015**, *15*, 15684–15716. [CrossRef] [PubMed]
176. Foster, H.A.; Ditta, I.B.; Varghese, S.; Steele, A. Photocatalytic disinfection using titanium dioxide: Spectrum and mechanism of antimicrobial activity. *Appl. Microbiol. Biotechnol.* **2011**, *90*, 1847–1868. [CrossRef] [PubMed]
177. Alhadrami, H.A.; Shoudri, R.A.M. Titanium oxide (TiO_2) nanoparticles for treatment of wound infection. *J. Pure Appl. Microbiol.* **2021**, *15*, 437–451. [CrossRef]
178. Nelson, B.C.; Johnson, M.E.; Walker, M.L.; Riley, K.R.; Sims, C.M. Antioxidant cerium oxide nanoparticles in biology and medicine. *Antioxidants* **2016**, *5*, 15. [CrossRef] [PubMed]
179. Chigurupati, S.; Mughal, M.R.; Okun, E.; Das, S.; Kumar, A.; McCaffery, M.; Seal, S.; Mattson, M.P. Effects of cerium oxide nanoparticles on the growth of keratinocytes, fibroblasts and vascular endothelial cells in cutaneous wound healing. *Biomaterials* **2013**, *34*, 2194–2201. [CrossRef] [PubMed]
180. Zamani, K.; Allah-Bakhshi, N.; Akhavan, F.; Yousefi, M.; Golmoradi, R.; Ramezani, M.; Bach, H.; Razavi, S.; Irajian, G.-R.; Gerami, M.; et al. Antibacterial effect of cerium oxide nanoparticle against Pseudomonas aeruginosa. *BMC Biotechnol.* **2021**, *21*, 68. [CrossRef] [PubMed]
181. Jin, T.; He, Y. Antibacterial activities of magnesium oxide (MgO) nanoparticles against foodborne pathogens. *J. Nanopart. Res.* **2011**, *13*, 6877–6885. [CrossRef]
182. Sawai, J.; Kojima, H.; Igarashi, H.; Hashimoto, A.; Shoji, S.; Sawaki, T.; Hakoda, A.; Kawada, E.; Kokugan, T.; Shimizu, M. Antibacterial characteristics of magnesium oxide powder. *World J. Microbiol. Biotechnol.* **2000**, *16*, 187–194. [CrossRef]
183. Salvo, J.; Sandoval, C. Role of copper nanoparticles in wound healing for chronic wounds: Literature review. *Burn. Trauma* **2021**, *10*, tkab047. [CrossRef] [PubMed]
184. *ISO 10993-1: 2025*; Biological Evaluation of Medical Devices. Part 1: Requirements and General Principles for the Evaluation of Biological Safety Within a Risk Management Process. International Organization for Standardization (ISO): Geneva, Switzerland, 2025.